Resolvent method for computations of localized defect modes of H-polarization in two-dimensional photonic crystals

Alexander Figotin and Vladimir Goren
Department of Mathematics, University of California, Irvine, California 92697
(Received 29 January 2001; published 30 October 2001)

We have developed and tested a version of the resolvent (or Green's function) method, based on the shift-inverse of the Maxwellian operator, that ensures stable convergence of iterative computations of localized defect modes of H-polarization in two-dimensional (2D) photonic crystals. The defect states are obtained by solving the eigenvalue problem for an associated compact operator with the expansion in Bloch eigenfunctions of the unperturbed Maxwellian operator. This method can be extended to 3D photonic crystals. We apply the method to a 2D square lattice of square dielectric rods in a dielectric background and compute (with controlled precision of $\sim 1\%$) the defect modes induced by the replacement of one rod (the defect). We investigate the rise and variation of the defect frequencies in a photonic band gap, caused by the increase of the dielectric strength of the defect, for four branches of localized modes of various symmetries.

DOI: 10.1103/PhysRevE.64.056623 PACS number(s): 42.70.Qs, 42.79.−e

I. INTRODUCTION

Photonic crystals (periodic dielectric structures) exhibiting gaps in the frequency spectrum of electromagnetic waves have attracted significant attention in recent years [1–5]. A problem of localized waves with frequencies arising in the gaps due to an isolated defect in a photonic crystal is of special importance [6,7]. Such modes, called defect modes, were observed experimentally for microwaves for a three-dimensional (3D) system [8], for 2D systems [9–11], and for a 1D system [9].

Photonic crystals with defects can be useful in a variety of devices such as resonators, filters, switches, waveguides, and more [2,4,5]. These applications require thorough theoretical analysis of conditions for the rise of a localized mode in a gap and of the dependence of its frequency and of the localization rate on the parameters of the photonic crystal.

Two-dimensional photonic crystals are of special interest [9]. Such structures are much easier to fabricate than 3D structures while they still allow many important applications. Theoretical analysis for 2D photonic crystals is significantly simpler than for 3D structures because a 2D dielectric system has two fundamental types of modes, E polarized and H polarized [12], for each of which the problem reduces to a one-component wave equation for E field or H field, respectively.

Analytical and numerical computations of the spectral system of a periodic dielectric structure with defects is a challenging problem. Analytical methods have been developed for 1D structures. The simplest configuration of such a layered system with a defect was studied using transfer matrix method [9,13], and a general configuration of a layered system was considered using propagation matrix method [14]. No analytical solution is known for 2D or 3D photonic crystals.

There have been three major approaches to numerical computations of the defect modes in photonic crystals: the supercell method, the time-domain integration, and the resolvent (or Green's function) method. The supercell method considers a finite region of a photonic crystal with a defect as a cell in a periodic superstructure. Combined with the plane-wave expansion, it has been applied to 3D [8,15] and 2D [16] systems, and the narrow frequency bands induced by defects have been obtained. The time-domain integration methods have been applied to simulate the excitation of E-polarized defect modes in 2D photonic crystals, using numerical solution of Maxwell's equations in a finite region with either periodic [17–19] or absorbing [20,21] boundary conditions.

The resolvent method (often called the Green's function method when used in the coordinate representation) gives an exact mathematical treatment of the defect modes in an infinite medium with a localized perturbation. It was first developed for electron systems described by Schrödinger's equation (see, for instance, [22]). In general, the spectral problem

$$\mathbf{A}\psi = \lambda\psi \tag{1}$$

is considered for a perturbed operator

$$\mathbf{A} = \mathbf{A}_0 + \mathbf{A}_1, \tag{2}$$

where the spectral system for the unperturbed operator $\mathbf{A}_0$ is known. The resolvent approach to finding the modes ψ with λ in the gaps of the spectrum of $\mathbf{A}_0$ (the defect states) is to recast the equation (1) with (2) as follows:

$$\mathbf{S}(\lambda)\psi = \psi, \tag{3}$$

$$\mathbf{S}(\lambda) = -(\mathbf{A}_0 - \lambda\mathbf{I})^{-1}\mathbf{A}_1, \tag{4}$$

where the first factor in $\mathbf{S}(\lambda)$ is called the resolvent operator for $\mathbf{A}_0$.

Numerical solution of the equation (3) for λ and ψ, where the space $\mathcal{L}$ of functions $\psi(\vec{r})$ is infinite dimensional, can be obtained using reduction of operator $\mathbf{S}$ to an N-dimensional subspace $\mathcal{L}_N$ of $\mathcal{L}$ and then increasing N to reach necessary precision for λ and ψ. (For example, this can be done using a discrete basis in $\mathcal{L}$ with increasing number N of functions retained for the matrix representation of $\mathbf{S}$.) Convergence of

such an iteration procedure is guaranteed only if **S** is a compact operator, that is, such operator (see items 1 and 2 of list in Sec. A 2) that its reduction to an N-dimensional subspace $\mathcal{L}_N$ converges normwise to the operator itself as $N\to\infty$ and $\mathcal{L}_N$ becomes the entire space $\mathcal{L}$.

For electrons in a crystal with a localized defect, Schrödinger's equation represents the spectral problem for a perturbed Hamiltonian operator, $\mathcal{H}=\mathcal{H}_0+\mathcal{H}_1$, where the unperturbed part includes differentiation of the second order, $\mathcal{H}_0=-a\,\Delta+U_0(\vec{r})$, where a is a constant, and the perturbation part is an operator of multiplication by a localized function, $\mathcal{H}_1=U_1(\vec{r})$. In this case (see Sec. A 1 a), the corresponding operator **S** (4) is compact.

For the electromagnetic field in a dielectric medium, the spectral problem for time-harmonic modes can be considered either with electric field $\vec{E}(\vec{r})$ for the operator $\mathbf{M}^E=\varepsilon^{-1}(\vec{r})\vec{\nabla}\times\vec{\nabla}\times$ or with magnetic field $\vec{H}(\vec{r})$ for the operator $\mathbf{M}^H=\vec{\nabla}\times\varepsilon^{-1}(\vec{r})\vec{\nabla}\times$, with an additional divergence free condition $\vec{\nabla}\cdot\varepsilon(\vec{r})\vec{E}(\vec{r})=0$ or $\vec{\nabla}\cdot\vec{H}(\vec{r})=0$, respectively. In either formulation, the perturbation operator $\mathbf{M}_1=\mathbf{M}-\mathbf{M}_0$, corresponding to a localized perturbation (defect) $\varepsilon_1(\vec{r})=\varepsilon(\vec{r})-\varepsilon_0(\vec{r})$ of the dielectric function, is also a second order differential operator, $\mathbf{M}_1^E=\gamma(\vec{r})\vec{\nabla}\times\vec{\nabla}\times$ or $\mathbf{M}_1^H=\vec{\nabla}\times\gamma(\vec{r})\vec{\nabla}\times$, where

$$\gamma(\vec{r})=\varepsilon^{-1}(\vec{r})-\varepsilon_0^{-1}(\vec{r})=-\varepsilon_1(\vec{r})/\varepsilon_0(\vec{r})\varepsilon(\vec{r}),$$

which balances the operator $\mathbf{M}_0$ in the resolvent factor [see Eq. (4)]. Because of that [see Sec. A 1 b (ii)], the corresponding operator **S** is not compact, and the convergence of numerical computations based on a straightforward application of the resolvent method to the operator **M** is not guaranteed [23,24].

Nevertheless, for E-field formulation, the perturbation term in the spectral equation can be represented as a result of multiplication by a localized function (like in Schrödinger's equation),

$$\mathbf{M}_1^E\vec{E}=\gamma(\vec{r})\vec{\nabla}\times\vec{\nabla}\times\vec{E}=\gamma(\vec{r})\varepsilon(\vec{r})\mathbf{M}^E\vec{E}$$
$$=-\varepsilon_1(\vec{r})\varepsilon_0^{-1}(\vec{r})\lambda\vec{E},$$

assuming $\vec{E}(\vec{r})$ is a solution of the spectral equation $\mathbf{M}^E\,\vec{E}=\lambda\vec{E}$. Therefore, the spectral problem for defect states can be represented in a form of Eq. (3) with a modified S operator, $\tilde{\mathbf{S}}(\lambda)=(\mathbf{M}_0^E-\lambda\mathbf{I})^{-1}\lambda\varepsilon_0^{-1}(\vec{r})\varepsilon_1(\vec{r})$, which is compact. Such resolvent approach (combined with the plane-wave expansion for the unperturbed spectral system) has been successfully implemented for a 1D layered medium [9,13] and for E-polarized modes in a 2D photonic crystal [25], where there is only one nonzero component of E field and no dependence on the corresponding coordinate so the divergence-free condition is satisfied automatically.

Similar resolvent approach with E-field formulation has been attempted for computations of defect states for H-polarized modes in a 2D photonic crystal [26]. However, because there are two nonzero components of E field depending on the same pair of coordinates, the divergence-free condition is not automatically satisfied. At the same time, an iteration procedure for numerical computations of λ and ψ, based on the expansion in eigenfunctions of the unperturbed operator $\mathbf{M}_0^E=\varepsilon_0^{-1}(\vec{r})\vec{\nabla}\times\vec{\nabla}\times$, with increasing number of the eigenfunctions retained, converges to functions satisfying the condition $\vec{\nabla}\cdot\varepsilon_0(\vec{r})\vec{E}(\vec{r})=0$ instead of the exact divergence-free condition $\vec{\nabla}\cdot\varepsilon(\vec{r})\vec{E}(\vec{r})=0$. The resolvent approach with E-field formulation to a 3D photonic crystal will face the same difficulty.

In this paper, we develop such version of the resolvent method with H-field formulation (see Sec. III A) that the corresponding operator **S** is compact. The approach is based on an equivalent representation of the spectral problem (1) for $\mathbf{M}^H$ in terms of the shift-inverse operator $(\mathbf{M}^H+m_s\mathbf{I})^{-1}$ [23,24]. We first implement this method for a 1D system (as a test) and then for H-polarized modes in a 2D photonic crystal, with the divergence-free condition being satisfied automatically (for H-field formulation). We observe stable convergence of the iteration procedure for computations of the defect states. The same version of the resolvent method with H-field formulation can be applied to a 3D photonic crystal (see Sec. A 1 b), where the divergence-free condition can be satisfied by using the expansion in eigenfunctions of the unperturbed periodic operator $\mathbf{M}_0^H$ [27].

II. BASIC EQUATIONS

The description of the dynamics of the electromagnetic field in a lossless dielectric medium can be reduced to the wave equation for the magnetic field $\vec{\mathrm{H}}(\vec{r},t)$,

$$c^{-2}\partial_t^2\vec{\mathrm{H}}=-\vec{\nabla}\times\frac{1}{\varepsilon(\vec{r})}\vec{\nabla}\times\vec{\mathrm{H}},\tag{5}$$

where c is the speed of light in vacuum and

$$\varepsilon(\vec{r})\geqslant 0,\tag{6}$$

with an additional divergence-free condition

$$\vec{\nabla}\cdot\vec{\mathrm{H}}(\vec{r},t)=0.\tag{7}$$

A. Two-dimensional system

We consider an infinite dielectric medium that is homogeneous along one axis (chosen to be the z axis), so the dielectric function depends on the two transversal coordinates only:

$$\varepsilon=\varepsilon(x,y).\tag{8}$$

For such a 2D medium, we consider here only such solutions of the vector wave equation (5) that depend on the two transversal coordinates only,

$$\vec{\mathrm{H}}=\vec{\mathrm{H}}(x,y;t),\tag{9}$$

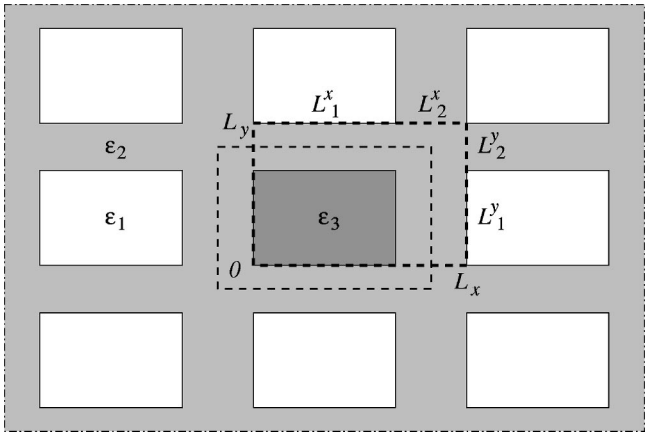

FIG. 1. A fragment of the cross section of a rectangular geometry 2D photonic crystal with a defect. The bold dashed rectangle shows a primitive cell chosen for computations; a lighter dashed rectangle shows a symmetric primitive cell.

representing electromagnetic waves propagating (or localized) in the x,y plane. There are two fundamental types of such solutions: H-polarized modes and E-polarized modes [12]. In this paper, we study H-polarized (or TE) modes where $\vec{\mathrm{H}}$ is parallel to the z axis,

$$\mathrm{H}_x = \mathrm{H}_y = 0. \tag{10}$$

For such solutions, the equation (5) reduces to the following scalar 2D wave equation for the z component of $\vec{\mathrm{H}}$:

$$c^{-2}\partial_t^2 \mathrm{H}_z = \left(\partial_x \frac{1}{\varepsilon(x,y)} \partial_x + \partial_y \frac{1}{\varepsilon(x,y)} \partial_y \right) \mathrm{H}_z, \tag{11}$$

where $-\infty < x,\ y < \infty$, and the condition (7) is satisfied identically.

We will consider a 2D periodic medium with a rectangular primitive cell and with a finite rectangular defect region. In terms of the dielectric function $\varepsilon(x,y)$ this can be represented as follows (choosing the axes of the cell to be the x axis and the y axis):

$$\varepsilon(x,y) = \varepsilon_0(x,y) + \varepsilon_1(x,y), \tag{12}$$

$$\varepsilon_0(x+L_x,y) = \varepsilon_0(x,y+L_y) = \varepsilon_0(x,y), \tag{13}$$

$$\varepsilon_1(x,y) \not\equiv 0,\ \ (x,y) \in (a_x,b_x) \times (a_y,b_y),$$

$$(b_x - a_x), (b_y - a_y) < \infty. \tag{14}$$

A simple configuration [Eqs. (96),(97)] of such a medium is shown in Fig. 1. In general, the resolvent method developed in this paper can be applied to an arbitrary configuration of a 2D periodic dielectric medium with a localized defect.

B. One-dimensional system

As a test system for our method, we consider an infinite dielectric medium where the dielectric function changes along one axis only (chosen to be the x axis),

$$\varepsilon = \varepsilon(x). \tag{15}$$

For such a 1D medium, we consider here only such solutions of the vector wave equation (5) that depend on the x coordinate only,

$$\vec{\mathrm{H}} = \vec{\mathrm{H}}(x,t), \tag{16}$$

and have a nonzero component along one transversal axis only (chosen to be the z axis for each such solution),

$$\mathrm{H}_x = \mathrm{H}_y = 0, \tag{17}$$

representing linear polarized electromagnetic waves propagating (or localized) along the x axis. For such a solution, the equation (5) reduces to the following scalar 1D wave equation for the z component of $\vec{\mathrm{H}}$:

$$c^{-2}\partial_t^2 \mathrm{H}_z = \partial_x \frac{1}{\varepsilon(x)} \partial_x \mathrm{H}_z, \tag{18}$$

where $-\infty < x < \infty$, and the condition (7) is satisfied identically.

We will study a periodic 1D medium of a period L with a defect of finite thickness. In terms of the dielectric function $\varepsilon(x)$ this can be represented as follows:

$$\varepsilon(x) = \varepsilon_0(x) + \varepsilon_1(x), \tag{19}$$

$$\varepsilon_0(x+L) = \varepsilon_0(x), \tag{20}$$

$$\varepsilon_1(x) \not\equiv 0,\ \ x \in (a,b),\ \ b-a < \infty. \tag{21}$$

C. Time-harmonic modes

We consider time-harmonic fields,

$$\mathrm{H}_z(\mathbf{r};t) = \psi(\mathbf{r}) \exp(-i\omega t) + \text{c.c.}, \tag{22}$$

$$\mathbf{r} = (x,y) \quad \text{for} \quad d=2, \quad \mathbf{r} = (x) \quad \text{for} \quad d=1, \tag{23}$$

for which the wave equation (11) or (18) reduces to the spectral problem for the d-dimensional scalar Maxwellian operator $\mathbf{M}$ (d denotes the number of dimensions for the system),

$$\mathbf{M}\psi(\mathbf{r}) = m\psi(\mathbf{r}) \tag{24}$$

with

$$m = (\omega/c)^2, \tag{25}$$

where

$$\mathbf{M} = -\sum_{\{\alpha\}} \partial_\alpha \frac{1}{\varepsilon(\mathbf{r})} \partial_\alpha, \tag{26}$$

$$\{\alpha\} = x,y \ \text{ for } \ d=2, \quad \{\alpha\} = x \ \text{ for } \ d=1, \tag{27}$$

is a non-negative self-adjoint operator in the space $L^2(\mathrm{R}^d)$ of functions $\psi(\mathbf{r})$ $(-\infty < r_\alpha < \infty)$ with the inner product

$$(\psi_1,\psi_2)=\int_{\mathrm{R}^d}\psi_1^*(\mathbf{r})\psi_2(\mathbf{r})\prod_{\{\alpha\}}dr_\alpha, \tag{28}$$

$$r_x=x,\quad r_y=y. \tag{29}$$

For a system of homogeneous regions where the dielectric function $\varepsilon(\mathbf{r})$ is piecewise constant, an operator of the form (26) can be understood in terms of the corresponding functional: given a function $\psi_2\in L^2(\mathrm{R}^d)$, the operator $\mathbf{M}$ defines the inner product

$$\begin{aligned}(\psi_1,\mathbf{M}\psi_2)&=\int_{\mathrm{R}^d}\psi_1^*(\mathbf{r})\left(-\sum_{\{\alpha\}}\partial_\alpha\frac{1}{\varepsilon(\mathbf{r})}\partial_\alpha\right)\psi_2(\mathbf{r})\prod_{\{\alpha\}}dr_\alpha\\&=\int_{\mathrm{R}^d}\frac{1}{\varepsilon(\mathbf{r})}\sum_{\{\alpha\}}[\partial_\alpha\psi_1^*(\mathbf{r})][\partial_\alpha\psi_2(\mathbf{r})]\prod_{\{\alpha\}}dr_\alpha\end{aligned} \tag{30}$$

with any function $\psi_1\in L^2(\mathrm{R}^d)$, provided the right-hand side exists with those functions $\psi_1(\mathbf{r})$ and $\psi_2(\mathbf{r})$.

According to the form (12)–(14) or (19)–(21) of the dielectric function, the Maxwellian operator $\mathbf{M}$ can be represented as a sum,

$$\mathbf{M}=\mathbf{M_0}+\mathbf{M}_1, \tag{31}$$

where

$$\mathbf{M_0}=-\sum_{\{\alpha\}}\partial_\alpha\frac{1}{\varepsilon_0(\mathbf{r})}\partial_\alpha \tag{32}$$

is a Maxwellian operator for an unperturbed periodic medium [see Eq. (20) or (13)] and

$$\mathbf{M}_1=-\sum_{\{\alpha\}}\partial_\alpha\gamma(\mathbf{r})\partial_\alpha \tag{33}$$

is the perturbation for the Maxwellian operator due to the defect, with

$$\gamma(\mathbf{r})=\frac{1}{\varepsilon(\mathbf{r})}-\frac{1}{\varepsilon_0(\mathbf{r})}=\frac{-\varepsilon_1(\mathbf{r})}{\varepsilon(\mathbf{r})\varepsilon_0(\mathbf{r})}\not\equiv 0 \quad \text{for} \quad \mathbf{r}\in D\equiv\prod_{\{\alpha\}}(a_\alpha,b_\alpha). \tag{34}$$

D. Structure of the spectral system for the periodic medium

For further reference, we remind here some facts of the spectral theory of periodic self-adjoint operators (see, e.g., [22]) applying it to the Maxwellian operator (32). The spectral problem for the periodic medium [with periods L_α, see Eq. (13) or (20)],

$$\mathbf{M_0}\psi_0(\mathbf{r})=m_0\psi_0(\mathbf{r}), \tag{35}$$

can be solved with piecewise differentiable continuous functions $\psi_0(\mathbf{r})$ that possess the Bloch property:

$$\psi_{\mathbf{k}}(\mathbf{r}+L_\alpha\mathbf{e}_\alpha)=e^{ik_\alpha}\psi_{\mathbf{k}}(\mathbf{r}), \tag{36}$$

$$\mathbf{k}=(k_x,k_y)\quad \text{for}\ d=2,\quad \mathbf{k}=(k_x)\ \text{for}\ d=1 \tag{37}$$

($\mathbf{e}_\alpha$ is a unit vector along an α axis). Such functions can be expressed in the form

$$\psi_{\mathbf{k}}(\mathbf{r})=e^{i\mathbf{q}\cdot\mathbf{r}}u_{\mathbf{k}}(\mathbf{r}),\quad q_\alpha=k_\alpha/L_\alpha, \tag{38}$$

$$u_{\mathbf{k}}(\mathbf{r}+L_\alpha\mathbf{e}_\alpha)=u_{\mathbf{k}}(\mathbf{r}), \tag{39}$$

representing modulated waves of $\mathrm{H}_z(\mathbf{r},t)$ [see Eq. (22)] propagating along the x,y plane for $d=2$ or along the x axis for $d=1$.

The spectral problem (35) for the operator $\mathbf{M}_0$ (32) with the condition (36) can be solved for each $\mathbf{k}$ separately, being reduced to one primitive cell Q,

$$\mathbf{M}_0\psi_{0\mathbf{k}}(\mathbf{r})=m_0(\mathbf{k})\psi_{0\mathbf{k}}(\mathbf{r}), \tag{40}$$

$$\mathbf{r}\in Q\equiv\prod_{\{\alpha\}}(0,L_\alpha], \tag{41}$$

where $\psi_{0\mathbf{k}}(\mathbf{r})$ has to satisfy the Bloch boundary conditions

$$\begin{aligned}&\psi_{0\mathbf{k}}(\mathbf{r}'+L_\alpha\mathbf{e}_\alpha)=e^{ik_\alpha}\psi_{0\mathbf{k}}(\mathbf{r}'),\\&\partial_\alpha\psi_{0\mathbf{k}}(\mathbf{r}'+L_\alpha\mathbf{e}_\alpha)=e^{ik_\alpha}\partial_\alpha\psi_{0\mathbf{k}}(\mathbf{r}'),\\&\mathbf{r}'=r_{\alpha'}\mathbf{e}_{\alpha'},\quad r_{\alpha'}\in(0,L_{\alpha'}],\quad \alpha'\neq\alpha.\end{aligned} \tag{42}$$

All values of $\mathbf{k}$ yielding different solutions of the eigenvalue problem (40)–(42) fill the Brillouin zone,

$$\mathbf{k}\in P\equiv[-\pi,\pi]^d. \tag{43}$$

According to Eqs. (28) and (36), any two Bloch functions with different $\mathbf{k}\in P$ are orthogonal,

$$(\psi_{1\mathbf{k}},\psi_{2\mathbf{k}'})=(2\pi)^d\delta(\mathbf{k}-\mathbf{k}')(\psi_{1\mathbf{k}},\psi_{2\mathbf{k}})_Q, \tag{44}$$

where

$$(\psi_1,\psi_2)_Q=\int_Q\psi_1^*(\mathbf{r})\psi_2(\mathbf{r})\prod_{\{\alpha\}}dr_\alpha \tag{45}$$

is the inner product in the space $L^2(Q)$ of functions $\psi(\mathbf{r})$ considered on one primitive cell Q.

For every fixed $\mathbf{k}$, the solution of the eigenvalue problem (40)–(42) forms a discrete system,

$$\{\psi_{0n,\mathbf{k}}(\mathbf{r}),m_0(n,\mathbf{k})\}\quad (n=1,2,\ldots,\infty), \tag{46}$$

$$m_0(n+1,\mathbf{k})\geqslant m_0(n,\mathbf{k}), \tag{47}$$

where n enumerates the eigenfunctions $\psi_{0n,\mathbf{k}}(\mathbf{r})$ in the ascending order of the corresponding eigenvalues $m_0(n,\mathbf{k})$, counting each multiple eigenvalue (if any) the number of times (in a row) equal to its multiplicity; there may be some multiple eigenvalues for a 2D system due to some extra symmetry (e.g., $L^x_{1,2}=L^y_{1,2}$), while for a 1D system there are no multiple eigenvalues (for the same $\mathbf{k}$). The set (46) of functions $\psi_{0n,\mathbf{k}}$ with the same $\mathbf{k}$ forms an orthogonal basis for $L^2(Q)$,

$$(\psi_{0n,\mathbf{k}},\psi_{0n',\mathbf{k}})_Q = C_d \delta_{n,n'}, \tag{48}$$

assuming that the set of linear independent eigenfunctions corresponding to the same multiple eigenvalue is chosen to be orthogonal.

Consequently, the solution of the spectral problem (35) for the periodic operator $\mathbf{M}_0$ in $L^2(\mathrm{R}^d)$ has the band structure

$$\{\psi_{0n,\mathbf{k}}(\mathbf{r}), m_0(n,\mathbf{k}) \mid \mathbf{k} \in P \equiv [-\pi,\pi]^d\} \quad (n=1,2,\ldots,\infty), \tag{49}$$

where n enumerates the bands; for each fixed n, the value $m_0(n,\mathbf{k})$ spans a spectral band when $\mathbf{k}$ spans the Brillouin zone.

The system (49) of Bloch eigenfunctions $\psi_{0n,\mathbf{k}}(\mathbf{r})$ forms an orthogonal basis in $L^2(\mathrm{R}^d)$ [see Eqs. (44) and (48)], which will be orthonormal,

$$(\psi_{0n,\mathbf{k}},\psi_{0n',\mathbf{k}'}) = \delta_{n,n'}\delta(\mathbf{k}-\mathbf{k}'), \tag{50}$$

if we choose

$$C_d = 1/(2\pi)^d. \tag{51}$$

For certain configurations of the periodic medium, there can be gaps between the spectral bands. Existence of gaps in the spectrum was proven in [28,29] (under certain conditions) for a 2D periodic medium of a rectangular geometry (as in Sec. IV B) and in [14] for a two-layer 1D periodic medium.

III. THE RESOLVENT METHOD

We are interested in the defect states that are such solutions of the spectral problem (24)–(26) for the perturbed operator $\mathbf{M}$ that the eigenvalues m are located in the gaps of the spectrum of the unperturbed operator $\mathbf{M}_0$ (32) and the eigenfunctions $\psi(\mathbf{r})$ are localized in $\mathbf{r}$ [24,30].

A. Formulation for the shift-inverse of the Maxwellian operator

To use the resolvent method for computations of the defect states (see Sec. I), we introduce the shift-inverse of the Maxwellian operator $\mathbf{M}$ (as proposed in [23,24]),

$$\mathbf{W} = (\mathbf{M} + m_s \mathbf{I})^{-1}, \tag{52}$$

where the shift by a constant

$$m_s > 0 \tag{53}$$

is necessary because the spectrum of the non-negative operator $\mathbf{M}$ (26) starts from zero; an optimal value of m_s (to be specified later) would be of order of width of the first spectral band. An S operator corresponding to the operator $\mathbf{W}$ will be compact while it would not be compact for the operator $\mathbf{M}$ itself (see Secs. I and A1 b). The eigenvalue problem for $\mathbf{W}$,

$$\mathbf{W}\psi(\mathbf{r}) = w\psi(\mathbf{r}) \tag{54}$$

with

$$w = (m + m_s)^{-1}, \tag{55}$$

is equivalent to the original spectral problem (24) in terms of $\mathbf{M}$.

We also introduce the shift-inverse for the unperturbed operator $\mathbf{M}_0$,

$$\mathbf{W}_0 = (\mathbf{M}_0 + m_s \mathbf{I})^{-1}, \tag{56}$$

and consider the perturbation of the operator $\mathbf{W}$,

$$\mathbf{W}_1 = \mathbf{W} - \mathbf{W}_0. \tag{57}$$

The spectral problem (54) with (55) for the defect states m_d, ψ_d in the gaps of the unperturbed spectrum,

$$m_d \notin \mathrm{Spectrum}(\mathbf{M}_0), \tag{58}$$

is equivalent to the following equation:

$$\mathbf{S}(m_d)\psi_d(\mathbf{r}) = \psi_d(\mathbf{r}), \tag{59}$$

where

$$\mathbf{S}(m) = -(\mathbf{W}_0 - w\mathbf{I})^{-1}\mathbf{W}_1. \tag{60}$$

The resolvent factor in $\mathbf{S}(m)$ can be represented in terms of the operator $\mathbf{M}_0$ and with an explicit dependence on m [see Eqs. (56) and (55)]:

$$(\mathbf{W}_0 - w\mathbf{I})^{-1} = -(m+m_s)(\mathbf{M}_0 - m\mathbf{I})^{-1}(\mathbf{M}_0 + m_s\mathbf{I}). \tag{61}$$

Solutions m_d, ψ_d of the equation (59) for the defect modes can be effectively found in the following way: first, we solve the eigenvalue problem

$$\mathbf{S}(\mu)\Psi(\mathbf{r};\mu) = s(\mu)\Psi(\mathbf{r};\mu) \tag{62}$$

for the operator $\mathbf{S}(\mu)$ with the parameter μ taking an arbitrary value in a gap of the unperturbed spectrum,

$$\mathbf{S}(\mu) = (\mu + m_s)(\mathbf{M}_0 - \mu\mathbf{I})^{-1}(\mathbf{M}_0 + m_s\mathbf{I})\mathbf{W}_1, \tag{63}$$

$$\mu \notin \mathrm{Spectrum}(\mathbf{M}_0); \tag{64}$$

then, we find the defect spectral values m_d from the equation

$$s(m_d) = 1; \tag{65}$$

finally, we obtain the defect modes ψ_d by substituting m_d for μ,

$$\psi_d(\mathbf{r}) = \Psi(\mathbf{r};m_d). \tag{66}$$

The equation (57) for the perturbation of the shift-inverse operator can be represented in the following form [see Eqs. (52), (56), and (31)]:

$$\mathbf{W}_1 = -\mathbf{W}\mathbf{M}_1\mathbf{W}_0. \tag{67}$$

Hence, a matrix or integral representation for the operator $\mathbf{W}_1$ can be effectively found by solving the following equation [see Eqs. (52) and (56)]:

$$(\mathbf{M}+m_s\mathbf{I})\mathbf{W}_1=-\mathbf{M}_1(\mathbf{M}_0+m_s\mathbf{I})^{-1}. \tag{68}$$

The operator $\mathbf{W}_1$ (67) is compact since it has two resolvent factors [see Eqs. (52) and (56)], with $\mathbf{M}$ (26) or $\mathbf{M}_0$ (32), versus one factor $\mathbf{M}_1$ (33) with a localized function $\gamma(\mathbf{r})$ (34) [see [23,24] and Sec. A 1 b (i)]. Consequently, the operator $\mathbf{S}(\mu)$ (63) is also compact and its spectrum is purely discrete [see Sec. A 1 b (i) and item (3) of list in Sec. A 2]. Therefore, the convergence of an iterative numerical solution (see Sec. I) is guaranteed for both the equation (68) for $\mathbf{W}_1$ and the equation (62) for the spectral system of $\mathbf{S}(\mu)$.

If the operator $\mathbf{M}_1$ (33) is sign definite [the simplest realization is where $\varepsilon_1(\mathbf{r})$ is sign definite, see Eq. (34)] then the self-adjoint operator $\mathbf{W}_1$ (57) is also sign definite with an opposite sign [due to Eqs. (52), (56), and (31)]. Hence, each eigenvalue $s(\mu)$ of the operator $\mathbf{S}(\mu)$ (63) is real and monotone in μ (within a gap of the spectrum of $\mathbf{M}_0$). This can be shown by reducing the equation (62) to the eigenvalue problem for a self-adjoint operator $\pm(\pm\mathbf{W}_1)^{1/2}\mathbf{S}(\mu)(\pm\mathbf{W}_1)^{-1/2}$ [see Eq. (63) and [23,24]] that is monotone in μ, increasing for positive $\mathbf{W}_1$ (upper sign) or decreasing for negative $\mathbf{W}_1$ (lower sign). Therefore, the equation (65) will have at most one solution m_d in each gap of the spectrum of $\mathbf{M}_0$ for each eigenvalue $s(\mu)$.

B. Bloch representation

It is convenient to take the system (49) of Bloch eigenfunctions of the operator $\mathbf{M}_0$ as a basis for the representation of the equations (62) and (68). An eigenfunction $\Psi(\mathbf{r};\mu)$ of the operator $\mathbf{S}(\mu)$ represents with its Fourier coefficients $\{a(n,\mathbf{k};\mu)\}$,

$$\Psi(\mathbf{r};\mu)=\sum_{n=1}^{\infty}\int_P a(n,\mathbf{k};\mu)\psi_{0n,\mathbf{k}}(\mathbf{r})\prod_{\{\alpha\}}dk_\alpha, \tag{69}$$

and the equation (62) yields the following system of integral equations for the coefficients $\{a(n,\mathbf{k};\mu)\}$:

$$\sum_{n'=1}^{\infty}\int_P S(n,\mathbf{k};n',\mathbf{k}';\mu)a(n',\mathbf{k}';\mu)\prod_{\{\alpha\}}dk'_\alpha = s(\mu)a(n,\mathbf{k};\mu),$$
$$n=1,2,\ldots,\infty,\quad k_\alpha\in[-\pi,\pi], \tag{70}$$

where

$$S(n,\mathbf{k};n',\mathbf{k}';\mu)=(\psi_{0n,\mathbf{k}},\mathbf{S}(\mu)\psi_{0n',\mathbf{k}'})=(\mu+m_s)(m_0(n,\mathbf{k})-\mu)^{-1}\times(m_0(n,\mathbf{k})+m_s)W_1(n,\mathbf{k};n',\mathbf{k}') \tag{71}$$

is the kernel matrix of the operator $\mathbf{S}(\mu)$ (63).

The equation (68) yields the following system of integral equations for the kernel matrix $W_1(n,\mathbf{k};n',\mathbf{k}')$ of the perturbation $\mathbf{W}_1$ of the shift-inverse operator:

$$\sum_{n'=1}^{\infty}\int_P M_1(n,\mathbf{k};n',\mathbf{k}')W_1(n',\mathbf{k}';n'',\mathbf{k}'')\prod_{\{\alpha\}}dk'_\alpha + (m_0(n,\mathbf{k})+m_s)W_1(n,\mathbf{k};n'',\mathbf{k}'') = -M_1(n,\mathbf{k};n'',\mathbf{k}'')(m_0(n'',\mathbf{k}'')+m_s)^{-1},$$
$$n,n''=1,2,\ldots,\infty,\quad k_\alpha,k''_\alpha\in[-\pi,\pi], \tag{72}$$

where Eq. (31) is taken into account and

$$M_1(n,\mathbf{k};n',\mathbf{k}')=(\psi_{0n,\mathbf{k}},\mathbf{M}_1\psi_{0n',\mathbf{k}'})=\int_D\gamma(\mathbf{r})\sum_{\{\alpha\}}(\partial_\alpha\psi^*_{0n,\mathbf{k}}(\mathbf{r}))\times(\partial_\alpha\psi_{0n',\mathbf{k}'}(\mathbf{r}))\prod_{\{\alpha\}}dr_\alpha \tag{73}$$

is the kernel matrix of the perturbation operator $\mathbf{M}_1$ [see Eqs. (33), (34), and (30)].

We would like to emphasize that the application of the resolvent method implies that the spectral system (49) for the unperturbed periodic operator $\mathbf{M}_0$ is found prior to the computation of the defect states. Some useful information on the current sate of the photonic band structure computations can be found in [36] and in references therein.

C. Numerical analysis

Solving the system (70), we find a function $s(\mu)$ on a grid of values μ within a gap and then solve the equation (65) for a defect spectral value m_d using an appropriate interpolation. We refine the grid to reach necessary precision for m_d.

The infinite system of homogeneous integral equations (70) is solved iteratively. We discretize the integration in k_α over $[-\pi,\pi]$, using an appropriate quadrature rule with the quadrature abscissas and weights $\{k_j,w_j\}$ $(j=1,2,\ldots,K)$ corresponding to the partition number K, and truncate the summation in n with a number N_1. For fixed K and N_1 we obtain, at each fixed value of μ within a gap, the following finite homogeneous system of linear algebraic equations for the unknown coefficients $\{a(n,\mathbf{k_j};\mu)\}$:

$$\sum_{n'=1}^{N_1}\sum_{\mathbf{j}'}S(n,\mathbf{k_j};n',\mathbf{k_{j'}};\mu)a(n',\mathbf{k_{j'}};\mu)\prod_{\{\alpha\}}w_{j'_\alpha} = s(\mu)a(n,\mathbf{k_j};\mu)\quad(j'_\alpha=1,2,\ldots,K),$$
$$n=1,2,\ldots,N_1,\ j_\alpha=1,2,\ldots,K, \tag{74}$$

$$\mathbf{j}=(j_x,j_y),\ \mathbf{k_j}=(k_{j_x},k_{j_y})\quad\text{for}\quad d=2,$$
$$\mathbf{j}=(j_x),\ \mathbf{k_j}=(k_{j_x})\quad\text{for}\quad d=1. \tag{75}$$

The system (74) forms the eigenvalue problem for the matrix $S(n,\mathbf{k_j};n',\mathbf{k_{j'}};\mu)\Pi_{\{\alpha\}}w_{j'_\alpha}$ (of a finite size N_1K^d) with eigenvectors $\{a(n,\mathbf{k_j};\mu)\}_{n,\mathbf{j}}$ and eigenvalues $s(\mu)$. We solve it using a specialized standard library routine.

Because the operator $\mathbf{S}(\mu)$ [the eigenvalue problem (62) for it is represented by the system (70)] is compact, its spectrum is discrete with zero being the only possible limit point [see item (3) of list in Sec. A 2], and any eigenvalue $s_q(\mu)$ of the truncated discretized system (74) (with fixed number q, where q enumerates the eigenvalues in descending order) approaches certain limit with the increase of K and N_1, as well as the corresponding eigenvector $\{a_q(n,\mathbf{k_j};\mu)\}_{n,\mathbf{j}}$ does (completed with zero components for smaller N_1 and K). We increase K and N_1 until reaching necessary precision for an eigenvalue of interest and for the corresponding eigenvector (the latter can be evaluated based on the norm of the difference between the iteration results). Then, the corresponding approximation for the eigenfunction of the operator $\mathbf{S}(\mu)$ associated with that eigenvalue can be obtained from Eq. (69):

$$\Psi_q(\mathbf{r};\mu)\approx\sum_{n=1}^{N_1}\sum_{\mathbf{j}} a_q(n,\mathbf{k_j};\mu)\psi_{0n,\mathbf{k_j}}(\mathbf{r})\prod_{\{\alpha\}} w_{j_\alpha} \quad (j_\alpha=1,2,\ldots,K). \tag{76}$$

To know the matrix $S(n,\mathbf{k_j};n',\mathbf{k_{j'}};\mu)$ in the left-hand side of the system (74), we need to find [see Eq. (71)] a square matrix $W_1(n,\mathbf{k_j};n',\mathbf{k_{j'}})$ $(n,n'=1,2,\ldots,N_1,\ j_\alpha,j'_\alpha=1,2,\ldots,K)$ by solving the system (72) with necessary precision.

The infinite system (72) of nonhomogeneous integral equations of the second kind is solved iteratively. We discretize the integration in k_α, using the same quadrature rule as for the system (70) with the same partition number K, and truncate the summation in n with a number $N_2\geqslant N_1$, where fixed N_1 is the number of bands retained in the system (74). For fixed N_2 and K we obtain the following finite nonhomogeneous system of linear algebraic equations for the entries of a rectangular matrix $W_1(n',\mathbf{k_{j'}};n'',\mathbf{k_{j''}})$ $(n'=1,2,\ldots,N_2,\ n''=1,2,\ldots,N_1,\ j'_\alpha,j''_\alpha=1,2,\ldots,K)$:

$$\sum_{n'=1}^{N_2}\sum_{\mathbf{j'}} A(n,\mathbf{k_j};n',\mathbf{k_{j'}})W_1(n',\mathbf{k_{j'}};n'',\mathbf{k_{j''}}) = B(n,\mathbf{k_j};n'',\mathbf{k_{j''}}) \quad (j'_\alpha=1,2,\ldots,K),$$

$$n=1,2,\ldots,N_2,\quad n''=1,2,\ldots,N_1,\quad j_\alpha,j''_\alpha=1,2,\ldots,K, \tag{77}$$

with the following square matrix of coefficients:

$$A(n,\mathbf{k_j};n',\mathbf{k_{j'}})=M_1(n,\mathbf{k_j};n',\mathbf{k_{j'}})\prod_{\{\alpha\}} w_{j'_\alpha} + (m_0(n,\mathbf{k_j})+m_s)\delta_{n,n'}\delta_{\mathbf{j},\mathbf{j'}}, \tag{78}$$

and with the following rectangular matrix in the right-hand side:

$$B(n,\mathbf{k_j};n'',\mathbf{k_{j''}})=-M_1(n,\mathbf{k_j};n'',\mathbf{k_{j''}})(m_0(n'',\mathbf{k_{j''}})+m_s)^{-1}. \tag{79}$$

We solve the system (77) using a specialized standard library routine. Then, we obtain the square matrix $W_1(n',\mathbf{k_{j'}};n'',\mathbf{k_{j''}})$ $(n',n''=1,2,\ldots,N_1,\ j'_\alpha,j''_\alpha=1,2,\ldots,K)$ [needed in the equation (74)] just as the square part (in n') of the solution matrix of the system (77). Because the operator $\mathbf{W}_1$ [an equation (68) for it is represented by the system (72)] is compact, the obtained square matrix with fixed N_1 approaches certain limit with the increase of N_2 and K. We increase N_2 and K until reaching necessary precision for the square matrix $W_1(n',\mathbf{k_{j'}};n'',\mathbf{k_{j''}})$ (that can be evaluated based on the norm of the difference between the iteration results).

Practically, we control the precision (with respect to iterations in N_1, N_2, and K) for the final result [based on the solution of the system (74)], which is a defect spectral value m_d [due to the equation (65) with the condition (58)] and a vector $\{a(n,\mathbf{k_j};m_d)\}_{n,\mathbf{j}}$ representing the corresponding eigenfunction $\psi_d(\mathbf{r})$ [see Eqs. (66) and (76)]; the precision for a vector $\{a(n,\mathbf{k_j};m_d)\}_{n,\mathbf{j}}$ can be evaluated based on the norm of the difference between the iteration results (completed with zero components for smaller N_1 and K).

The computation of the kernel-matrix $M_1(n,\mathbf{k};n',\mathbf{k'})$ (73) involves differentiation and integration in r_α of oscillating functions $\psi_{0n,\mathbf{k}}(\mathbf{r})$ (the higher the n, the faster the oscillations). To efficiently carry out the computations, we need the eigenfunctions $\psi_{0n,\mathbf{k}}(\mathbf{r})$ of the unperturbed periodic operator $\mathbf{M}_0$ to be found (with necessary precision) in the form of superposition of a moderate number of analytically known functions.

IV. APPLICATION TO CERTAIN MEDIA

A. Layered one-dimensional system

As a test system for the resolvent method, we consider the simplest periodic medium of the type (19)–(21) with two homogeneous layers (of thickness L_1 and L_2) of different dielectric materials in the period cell (of thickness $L=L_1+L_2$), where one cell is replaced with a homogeneous layer of a third dielectric material. For such a configuration, the dielectric function (19)–(21) specifies as follows:

$$\varepsilon_0(x)=\epsilon_1,\quad x\in(0,L_1),$$

$$\varepsilon_0(x)=\epsilon_2,\quad x\in(L_1,L), \tag{80}$$

$$\varepsilon_1(x)=\epsilon_3-\varepsilon_0(x)\not\equiv 0,\quad x\in(0,L). \tag{81}$$

For such a system, we have obtained analytically the solution for both the unperturbed and the perturbed eigenvalue problems using the propagation matrix method [14]. We find it convenient to represent the spectrum (25) of the Maxwellian operator (26) in terms of the dimensionless frequency ν, as follows:

$$\nu=L_1\sqrt{\epsilon_1 m}=n_1L_1\omega/c, \tag{82}$$

where $n_i=\sqrt{\epsilon_i}$ is the refractive index of a dielectric material.

TABLE I. Results of computations of the gap edges and the defect states (in terms of the dimensionless frequency $\nu=\omega n_1 L_1/c$) for the first three gaps for a 1D system at $L_2/L_1=0.5$, $n_2/n_1=2.5$, and $n_3/n_1=3.5$ ($n_i=\sqrt{\epsilon_i}$). n_g is the gap number, (ν_l,ν_u) is the gap interval, ν_d is the defect frequency (PMM and RM stand for the propagation matrix method and for the resolvent method, respectively). For the resolvent method, K is a partition number for discrete integration in k, Δ_K is the corresponding evaluated absolute error for ν_d, N_1 or N_2 is the number of bands retained in Eq. (74) or Eq. (77), respectively, Δ_1 or Δ_2 is a corresponding evaluated absolute error for ν_d.

n_g	ν_l and ν_u	ν_d, PMM	ν_d, RM	K	Δ_K	N_1	Δ_1	N_2	Δ_2
1	1.006	1.084	1.086	10	0.0003	10	0.0002	60	0.0008
	1.780	1.442	1.444	8	−0.0004	10	0.0005	80	0.0009
2	2.667	2.807	2.813	12	0.0013	15	0.0008	80	0.0023
	2.929								
3	3.842	3.976	3.980	8	−0.0024	20	0.0014	100	0.0030
	4.518	4.332	4.342	8	0.0015	20	0.0018	100	0.0038

1. Analytical solution of the spectral problem for the periodic medium

The spectrum $\{m_0\}$ of the unperturbed 1D operator $\mathbf{M}_0$ (32) is given by the following equation for the corresponding frequency variable ν_0 [see Eq. (82)]:

$$\eta(\nu_0)=\cos(k), \quad -\pi\leqslant k\leqslant\pi, \tag{83}$$

where

$$\eta(\nu)=\cos(\nu)\cos(r\nu)-p\sin(\nu)\sin(r\nu), \tag{84}$$

$$p=(\rho+\rho^{-1})/2, \quad r=\rho\Lambda, \quad \rho=n_2/n_1, \quad \Lambda=L_2/L_1,$$

$$n_i=\sqrt{\epsilon_i}. \tag{85}$$

Using the phase-amplitude representation for $\eta(\nu)$ [14], we have shown that the frequency spectrum has bands $\{\nu_{0n}(k), k\in[-\pi,\pi]\}$ $(n=1,2,\dots)$ with a gap between each two consecutive bands. We can find $\nu_{0n}(k)$ for any n solving the equation (83) numerically.

The corresponding Bloch eigenfunctions $\psi_{0n,k}(x)$ can be easily found by solving the one-dimensional equation (40) [see Eq. (32)] on a one-cell interval $[0,L]$ with the Bloch boundary conditions (42),

$$\psi_{0n,k}(x)=\sigma_n(k)\breve{\psi}_{0n,k}(\breve{x})/\sqrt{L_1}, \quad \breve{x}=x/L_1, \quad L/L_1=1+\Lambda, \tag{86}$$

$$\breve{\psi}_{0n,k}(\breve{x})=[\eta_2(\nu)\cos(\nu\breve{x})+\{e^{ik}-\eta_1(\nu)\}\sin(\nu\breve{x})], \quad 0\leqslant\breve{x}\leqslant 1, \tag{87}$$

$$=[\eta_2(\nu)\cos(\nu)+\{e^{ik}-\eta_1(\nu)\}\sin(\nu)]\times\cos[\rho\nu(\breve{x}-1)]+\rho[-\eta_2(\nu)\sin(\nu)+\{e^{ik}-\eta_1(\nu)\}\cos(\nu)]\sin[\rho\nu(\breve{x}-1)], \quad 1\leqslant\breve{x}<1+\Lambda, \tag{88}$$

$$\eta_1(\nu)=\cos(\nu)\cos(r\nu)-\rho\sin(\nu)\sin(r\nu),$$

$$\eta_2(\nu)=\sin(\nu)\cos(r\nu)-\rho\cos(\nu)\sin(r\nu), \tag{89}$$

$$\nu=\nu_{0n}(k). \tag{90}$$

The constant $\sigma_n(k)$ (which can be taken as real-valued) is determined by the condition (51) [see Eqs. (48) and (45)]:

$$\frac{1}{\sigma_n(k)^2}=2\pi\int_0^{1+\Lambda}d\breve{x}|\breve{\psi}_{0n,k}(\breve{x})|^2. \tag{91}$$

Results of computations of edges for the first three gaps (in terms of the frequency variable ν) are shown in Table I for $L_2/L_1=0.5$ and $n_2/n_1=2.5$.

2. Computation of the defect states

(a) Resolvent approach. Introducing a one-cell defect as in Eq. (81), we look for the defect states m_d in the first three gaps, applying the resolvent method as described in Sec. III C. We consider $\epsilon_3\geqslant\max(\epsilon_1,\epsilon_2)$ so the perturbation function $\gamma(x)$ is negative and, consequently, each eigenvalue $s(\mu)$ of the operator $\mathbf{S}(\mu)$ is real and increasing function of μ (see end of Sec. III A). Because the width of the first spectral band of the operator $\mathbf{M}_0$ is close to 1 in terms of the frequency variable ν (see Table I), we take such value for the shift constant m_s [see Eqs. (52) and (53)] that corresponds to $\nu=1$ [see Eq. (82)],

$$m_s=1/\epsilon_1 L_1^2. \tag{92}$$

We compute the perturbation matrix $M_1(n,k;n',k')$ (73) analytically, using the formulas (86)–(90) for the Bloch functions $\psi_{0n,k}(x)$. The unperturbed frequency spectrum $\nu_{0n}(k)$ is computed by solving the equation (83) with (84) numerically (with relative precision of $\sim 10^{-10}\%$).

We observe a close to exponential convergence of computations of the defect frequencies ν_d [see Eq. (82)] with respect the increase of the numbers N_1 and N_2 of bands used in the equations (74) and (77), respectively, and of the partition number K (using the midpoint rule for the discrete integration in k). Results of computations of the defect frequencies ν_d in the first three gaps at $L_2/L_1=0.5$, n_2/n_1

$=2.5$, and $n_3/n_1=3.5$ are shown in Table I. These values ν_d are obtained at such N_1, N_2, and K (also shown) that the corresponding evaluated (based on the exponential convergence) error becomes $\sim 1\%$ (or less). For higher gaps, the number N_1 of bands retained in the equation (74) should be increasingly higher for the same relative precision for ν_d, but the number N_2 of bands retained in the equation (77) increases relatively less (while N_2 is much greater than N_1). For the same relative precision for ν_d, the partition number K for the discrete integration over k in the equations (74) and (77) should be larger when ν_d is close to one edge (first ν_d in the first gap) or to both edges (ν_d in the second gap) of the gap.

(b) Comparison with the analytical solution. In [14], we obtained the analytical solution using the propagation matrix method. The spectrum $\{m\}$ of the perturbed operator $\mathbf{M}$ consists of the continuous part coinciding with the spectrum $\{m_0\}$ of the unperturbed operator $\mathbf{M}_0$ and of the discrete set of defect eigenvalues $\{m_d\}$ located in the gaps of $\{m_0\}$ [where $|\eta(\nu)|>1$, see Eq. (84)] which is given by the following equation for the defect frequency ν_d [see Eq. (82)]:

$$\chi(\nu_d)=\mathrm{sgn}(\eta(\nu_d))\sqrt{\eta(\nu_d)^2-1}, \tag{93}$$

where

$$\chi(\nu)=\tan(v\nu)[q_1\sin(\nu)\cos(r\nu)+q_2\cos(\nu)\sin(r\nu)], \tag{94}$$

$$v=\sigma_1(1+\Lambda), \quad q_i=(\sigma_i+\sigma_i^{-1})/2, \quad \sigma_i=n_3/n_i,$$

$$n_i=\sqrt{\epsilon_i}. \tag{95}$$

We have shown [14] that there is at least one defect eigenvalue in each gap and one more for each point $\nu'_m=m\pi/v$ $(m=1,2,3,\ldots)$ appearing in the gap. We can find all defect eigenvalues in any gap by solving the equation (93) numerically. Results of computations (with the precision of $\sim 10^{-10}\%$) of the defect spectral values in the first three gaps (in terms of the frequency variable ν) are shown in Table I for $L_2/L_1=0.5$, $n_2/n_1=2.5$, and $n_3/n_1=3.5$. Comparing the results of computations of ν_d by the resolvent method with the ''exact'' results of the propagation matrix method, we find that the difference between them is at most two times greater than the total evaluated (based on the exponential convergence) error ($\Delta=\Delta_K+\Delta_1+\Delta_2$) for ν_d.

B. Rectangular geometry two-dimensional system

We consider a simple periodic medium of the type (12)–(14) consisting (see Fig. 1) of a rectangular lattice formed by rectangular rods with dimensions L_1^x and L_1^y of one dielectric, spaced by L_2^x and L_2^y, respectively, and of the grid of another dielectric filling the space between the rods. One rod is then replaced with a third dielectric forming a defect. For such a medium, the dielectric function (12)–(14) can be specified as follows:

$$\varepsilon_0(x,y)=\epsilon_1, \quad (x,y)\in(0,L_1^x)\times(0,L_1^y),$$

$$\varepsilon_0(x,y)=\epsilon_2, \quad (x,y)\in(0,L_x)\times(0,L_y)\backslash(0,L_1^x)\times(0,L_1^y), \tag{96}$$

$$\varepsilon_1(x,y)=\epsilon_3-\epsilon_1\not\equiv 0, \quad (x,y)\in(0,L_1^x)\times(0,L_1^y), \tag{97}$$

where the dimensions of a primitive cell (shown with the bold dashed rectangle in Fig. 1) are

$$L_x=L_1^x+L_2^x, \quad L_y=L_1^y+L_2^y. \tag{98}$$

We will represent the spectrum (25) of the Maxwellian operator (26) in terms of the dimensionless frequency ν [similarly to Eq. (82)],

$$\nu=L_1^x\sqrt{\epsilon_1 m}=n_1L_1^x\omega/c, \tag{99}$$

where $n_i=\sqrt{\epsilon_i}$ is the refractive index of a dielectric material.

In this paper, we do the computations for the case of a square geometry primitive cell,

$$L_{1,2}^x=L_{1,2}^y, \tag{100}$$

taking the following values for the relative thickness of the wall of the grid [see Eq. (A25)] and for the dielectric contrast between the wall and the rod [see Eq. (96)]:

$$\Lambda=L_2/L_1=0.1, \quad n_2/n_1=4 \quad (n_i=\sqrt{\epsilon_i}). \tag{101}$$

1. Computation of the spectral system for the periodic medium

We compute the spectral system (49) for the periodic operator $\mathbf{M}_0$ using the expansion in eigenfunctions of the auxiliary operator $\tilde{\mathbf{M}}_0$ as described in Sec. A 3. We test the convergence of these computations with respect to the increase of the number N_3 of eigenfunctions of $\tilde{\mathbf{M}}_0$ retained in the representation (A38) of the eigenvalue problem for the periodic medium. For the eigenvalues $m_0(n,\mathbf{k})$ in each nth band of the spectrum of $\mathbf{M}_0$, we monitor an average (over $k_{x,y}\in[-\pi,\pi]$ with a uniform partition with a number K) relative difference between consecutive iterations in N_3 with a fixed step and observe a close to exponential convergence. The minimal value N_3' that provides an average precision (an evaluated average relative error) of 1% or less for eigenvalues in each of the first N_2 bands of $\mathbf{M}_0$ (needed for the application of the resolvent method, see Sec. III C) is found to be approximately proportional to N_2 with a coefficient less than 10 (with any tested partition number K from 4 to 10):

$$N_3'\approx 7N_2, \quad 10\leqslant N_2\leqslant 100. \tag{102}$$

We find a wide gap between the first and the second spectral bands of $\mathbf{M}_0$. Computing the gap edges at increasing values of the truncation number N_3 and the partition number K, we observe a close to exponential convergence. An evaluated error with respect to N_3 is $\sim 0.1\%$ for the lower edge and $\sim 1\%$ for the upper edge of the gap at $N_3=10$, which is consistent with Eq. (102). Results of computations of the edges of the gap at increasing values of the number K for uniform partition at $N_3=40$ (providing the precision of $\sim 0.1\%$ or less with respect to N_3) are shown in Table II.

TABLE II. Results of computations of edges ν_l, ν_u (in terms of the dimensionless frequency $\nu=\omega n_1 L_1/c$) for the first spectral gap for a 2D photonic crystal with $L_2/L_1=0.5$ and $n_2/n_1=2.5$ ($n_i=\sqrt{\epsilon_i}$) at various values of the partition number K with the truncation number $N_3=40$; $d\nu_{l,u}$ is the difference between values of $\nu_{l,u}$ for the current and the next iteration, $\delta\nu_{l,u}$ is an evaluated relative error corresponding to the current value of K.

K	ν_l	$d\nu_l, 10^{-3}$	$\delta\nu_l$,%	ν_u	$d\nu_u, 10^{-3}$	$\delta\nu_u$,%
4	1.744	−126	−12	2.828	89	5.4
6	1.870	−49	−4.5	2.739	33	2.0
8	1.919	−23	−2.0	2.706	16	1.0
10	1.942			2.690		

2. Computation of the perturbation matrix

The perturbation matrix $M_1(n,\mathbf{k};n',\mathbf{k}')$ $(n,n'=1,2,\ldots,N_2)$ (73) which is needed for the application of the resolvent method [see Eqs. (77)–(79)] is computed based on the expansion (A43) for the eigenfunctions of the operator $\mathbf{M}_0$ in terms of eigenfunctions of the auxiliary operator $\tilde{\mathbf{M}}_0$ (see Sec. A 3),

$$\psi_{0n,\mathbf{k}}(x,y)\approx\sum_{\tilde{n}=1}^{N_3'} b_{n,\mathbf{k}}(\tilde{n})\tilde{\psi}_{0\tilde{n},\mathbf{k}}(x,y),\quad n=1,2,\ldots,N_2, \tag{103}$$

where the truncation number N_3' is such [see Eq. (102)] that it provides necessary precision (of $\sim 1\%$) for the first N_2 bands of $\mathbf{M}_0$ (see Sec. IV B 1). Then, the perturbation matrix represents as follows:

$$M_1(n,\mathbf{k};n',\mathbf{k}') \approx\sum_{\tilde{n}=1}^{N_3'}\sum_{\tilde{n}'=1}^{N_3'} b^*_{n,\mathbf{k}}(\tilde{n})b_{n',\mathbf{k}'}(\tilde{n}')\tilde{M}_1(\tilde{n},\mathbf{k};\tilde{n}',\mathbf{k}'), \quad n,n'=1,2,\ldots,N_2, \tag{104}$$

where we introduce the matrix of the perturbation operator $\mathbf{M}_1$ with respect to the basis system of eigenfunctions of the auxiliary operator $\tilde{\mathbf{M}}_0$,

$$\tilde{M}_1(\tilde{n},\mathbf{k};\tilde{n}',\mathbf{k}')=(\tilde{\psi}_{0\tilde{n},\mathbf{k}},\mathbf{M}_1\tilde{\psi}_{0\tilde{n}',\mathbf{k}'}) =\int_0^{L_1^x}dx\int_0^{L_1^y}dy\,\gamma(x,y)\sum_{\alpha=x,y}(\partial_\alpha\tilde{\psi}^*_{0\tilde{n},\mathbf{k}}(x,y))\times(\partial_\alpha\tilde{\psi}_{0\tilde{n}',\mathbf{k}'}(x,y)) \tag{105}$$

[see Eqs. (33), (34), and (97)], which can be computed analytically [see Eq. (A30)].

3. Computation of the defect states

Introducing a one-rod defect as in Eq. (97) with a dielectric constant ϵ_3, we look for defect sates m_d in the first gap at increasing values of the defect-medium dielectric contrast n_3/n_1 ($n_i=\sqrt{\epsilon_i}$), applying the resolvent method as described in Sec. III C. We consider $\epsilon_3\geqslant\epsilon_1$, so the perturbation function $\gamma(x,y)$ is negative and, consequently, each eigenvalue $s(\mu)$ of the operator $\mathbf{S}(\mu)$ is a real and increasing function of μ (see end of Sec. III A). Because the width of the first spectral band of the operator $\mathbf{M}_0$ is of order of one in terms of the frequency variable ν (see Table II), we take such value for the shift constant m_s [see Eqs. (52) and (53)] that corresponds to $\nu=1$ [see Eq. (99)]:

$$m_s=1/\epsilon_1(L_1^x)^2. \tag{106}$$

Four branches of the defect states are found for values of n_3/n_1 within the interval [1.0,3.5] (see Fig. 2).

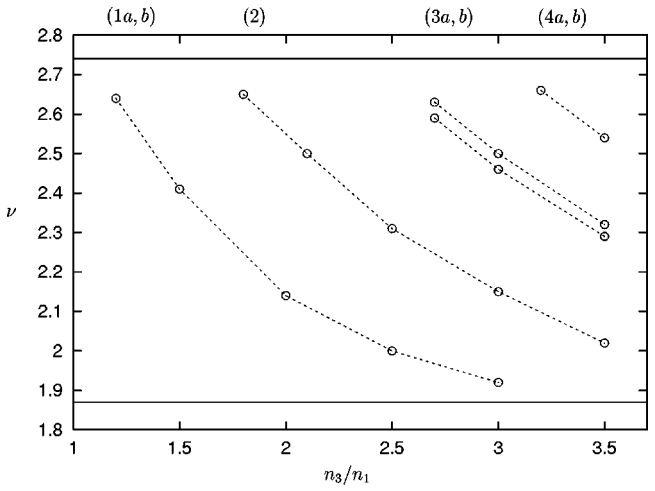

FIG. 2. Dimensionless frequencies ν_d ($\nu=\omega n_1 L_1/c$) for the first four branches of localized defect modes [doublet (1a,b and 4a,b), singlet (2), and quasidoublet (3a,b) states] at increasing values of the defect-medium dielectric contrast n_3/n_1 ($n_i=\sqrt{\epsilon_i}$) for a 2D square lattice of square dielectric rods in a dielectric background with a one-rod replacement defect (see Fig. 1) at $L_2/L_1=0.1$ and $n_2/n_1=4.0$.

We test the convergence of computations of the defect frequencies ν_d [see Eq. (99)] with respect to the increase of the truncation numbers N_1 [for the bands used in the eigenvalue equation (74) for the operator $\mathbf{S}$] and N_2 [for the bands used in the equation (77) for the perturbation operator $\mathbf{W}_1$] and of the partition number K [using the midpoint rule for the discrete integration in k_α in Eqs. (74) and (77)]. Results of such computations for the defect frequency ν_2 of the second branch at $n_3/n_1=2.5$ are presented in Table III, showing a close to exponential convergence with respect to each of the numbers N_1, N_2, and K.

We compute the defect frequencies at increasing values of the contrast n_3/n_1. For each defect state at each value of n_3/n_1, we increase N_1, N_2, and K until an evaluated (based on the exponential hypothesis) error for the defect frequency becomes 1% or less. For each iteration, we take the value of the truncation number N_3 [for the bands of the auxiliary operator $\tilde{\mathbf{M}}_0$ used in the equation (A38) for the spectrum of the operator $\mathbf{M}_0$] to be at least N_3' (102) providing the precision of 1% for the first N_2 bands of $\mathbf{M}_0$.

TABLE III. Results of computations of the dimensionless frequency ν_2 ($\nu=\omega n_1 L_1/c$) in the second defect state branch for a 2D photonic crystal at $n_3/n_1=2.5$ ($n_i=\sqrt{\epsilon_i}$) at increasing values of one of the truncation numbers N_1 and N_2 or of the partition number K while the other two are fixed [and the number $N_3'=350$, see Eq. (102)]; $d\nu_2$ is the difference between values of ν_2 for the current and the next iteration, $\delta\nu_2$ is an evaluated relative error corresponding to the current value of the number (N_1, or N_2, or K) being iterated.

N_1	N_2	K	ν_2	$d\nu_2, 10^{-3}$	$\delta\nu_2$,%
20	40	4	2.2865	2.7	0.14
		6	2.2838	0.5	0.03
		8	2.2833	0.1	
		10	2.2832		
20	20	6	2.3343	44	1.3
	30		2.2907	7.0	0.48
	40		2.2838	2.6	0.15
	50		2.2811		
10	40	6	2.2982	15	0.85
20			2.2837	6.4	0.31
30			2.2773	1.0	
40			2.2763		

The values of N_1 and N_2 that provide the precision (the corresponding evaluated error) $\delta_{1,2}\sim 1\%$ are shown in Table IV for some of the defect frequencies. We find that computations of the defect states at higher values of the defect-medium dielectric contrast n_3/n_1 require higher numbers N_1 and N_2 for the same precision. This can be related to higher spatial oscillations of a defect eigenfunction localized in the vicinity of the defect with higher dielectric constant ϵ_3 (which can be roughly thought of as eigenfunctions of an operator $\epsilon_3^{-1}\Delta$ in the defect region; see [30]) so an expansion of this function in Bloch waves should involve higher bands of the periodic operator $\mathbf{M}_0$.

TABLE IV. Values of the truncation numbers N_1 and N_2 that provide the corresponding precision $\delta_{1,2}\sim 1\%$ (or less) for the dimensionless frequencies ν_d ($\nu=\omega n_1 L_1/c$) of the defect states in the first gap, $1.87<\nu<2.74$ at some values of the defect-medium dielectric contrast n_3/n_1 ($n_i=\sqrt{\epsilon_i}$) for a 2D photonic crystal. Computations of the defect frequencies ν_d are performed at those values N_1 and N_2 and at the partition number $K=6$. Corresponding evaluated errors δ_1, δ_2, and δ_K are also shown.

n_3/n_1	ν_d	branch	N_1	δ_1,%	N_2	δ_2,%	δ_K,%
1.5	2.41	$1_{a,b}$	5	0.38	10	0.15	0.11
2.5	2.00	$1_{a,b}$	10	0.47	30	0.89	0.14
	2.31	2	10	0.85	30	0.48	0.02
3.5	2.02	2	20	1.1	50	0.53	0.03
	2.29	3_a	30	1.0	60	0.61	−0.39
	2.32	3_b	30	0.64	60	1.2	0.15
	2.54	$4_{a,b}$	30	0.95	50	0.49	0.37

TABLE V. Values of the partition number K that provide the precision (the corresponding evaluated relative error) $\delta_K\sim 1\%$ (or less) for some values of the dimensionless frequencies ν_d ($\nu=\omega n_1 L_1/c$) of the defect states at certain values of n_3/n_1 ($n_i=\sqrt{\epsilon_i}$) in each of the first three branches in the first gap, $1.87<\nu<2.74$, for a 2D photonic crystal; δ_K itself is also shown. Computations are performed at such values of the truncation numbers N_1 and N_2 that provide corresponding precision $\delta_{1,2}\sim 1\%$ (or less).

n_3/n_1	ν_1	K	δ_K,%	n_3/n_1	ν_2	K	δ_K,%
1.2	2.64	6	0.65	1.8	2.65	4	0.63
1.5	2.41	6	0.11	2.5	2.31	4	0.10
3.0	1.92	6	−2.4	3.5	2.03	4	0.12
n_3/n_1	ν_{3a}	K	δ_K,%	n_3/n_1	ν_{3b}	K	δ_K,%
2.7	2.59	6	−0.25	2.7	2.63	6	0.75
3.5	2.29	6	−0.39	3.5	2.32	6	0.15

The values of K that provide the precision (the corresponding evaluated error) $\delta_K\sim 1\%$, as well as δ_K itself, are shown in Table V for some defect frequencies in each of the first three defect branches in the first gap. For the same branch, the error at the same value of K is higher for frequencies that are closer to the gap edge.

Results of computations of the defect frequencies at increasing values of the defect-medium dielectric contrast n_3/n_1 (starting from the value 1.0 for the unperturbed medium) are shown in Fig. 2. We find that the first defect frequency arises at the upper edge of the gap immediately, as soon as $n_3>n_1$, while the second defect frequency arises at $n_3/n_1\approx 1.5$. When the defect-medium dielectric contrast n_3/n_1 increases, the defect frequencies decrease, to finally vanish at the lower edge of the gap. (We estimate that the first defect state should vanish at $n_3/n_1\approx 3.5$). Such behavior is consistent with the general analysis [23,24] based on the properties of the operator $\mathbf{S}(\mu)$.

We have to note certain multiplicity of the defect eigenfrequency in each of the four investigated branches and its relation to certain symmetry of the corresponding eigenfunctions. For a rectangular geometry periodic medium with a rectangular defect that is concentric with a symmetric primitive cell (see Fig. 1), both the unperturbed operator $\mathbf{M}_0$ and the perturbed operator $\mathbf{M}$ have an orthogonal symmetry: they are invariant with respect to the reflection about each of the two mid-lines,

$$(x-x_0)\leftrightarrow(x_0-x) \quad \text{or} \quad (y-y_0)\leftrightarrow(y_0-y), \tag{107}$$

where (x_0,y_0) is the center of the defect. For the particular case of the square geometry (100) for which we did the computations, there is an additional symmetry with respect to the diagonal reflection,

$$(x-x_0)\leftrightarrow(y-y_0). \tag{108}$$

Invariance of an operator with respect to both types of reflection, (107) and (108), constitutes a tetragonal symmetry. Such a symmetry of an operator allows two situations con-

cerning the multiplicity of its eigenvalues and the related to it symmetry of the corresponding eigenfunctions (see, e.g., [31]). One case is a singlet state where an eigenvalue is of multiplicity 1 and the corresponding eigenfunction has a tetragonal symmetry. The other case is a doublet state where an eigenvalue is of multiplicity 2 and two corresponding basis eigenfunctions can be chosen to have each (at most) an orthogonal symmetry while the pair being symmetric with respect to the diagonal reflection.

Results of our computations are consistent with the general symmetry analysis. The first, lowest branch of the defect states is a doublet: we find a pair of basis eigenfunctions (1a and 1b) with the same (up to 14 digits) corresponding eigenfrequency ν_1, both having orthogonal symmetry (of opposite signs). The second branch is a singlet: we see one eigenfunction having a tetragonal symmetry, which corresponds to a solitary eigenfrequency ν_2. We identify as a third branch a pair of singlet states (3a and 3b) where both eigenfunctions have a tetragonal symmetry [of opposite signs with respect to the diagonal reflection (108)] while the corresponding eigenfrequencies (ν_{3a} and ν_{3b}) differ by only about 2%; such a pair of states can be called quasidoublet (see [31]) and thought of as a result of splitting of a doublet state of a hypothetical operator with an octagonal (higher) symmetry caused by the actual operator **M** having a tetragonal (lower) symmetry. The fourth branch is a doublet (4a and 4b) with an eigenfrequency ν_4 (similarly to the first one).

V. CONCLUSIONS

We have developed a version of the resolvent method that guarantees a stable convergence of the iterative computations of localized defect modes of H polarization in 2D photonic crystals and allows us to control the computational precision. It is based on an equivalent representation of the spectral problem in terms of the shift-inverse of the Maxwellian operator. The defect states are obtained by solving the eigenvalue equation for an associated compact operator with the expansion in Bloch eigenfunctions of the unperturbed Maxwellian operator. This method can be also extended to 3D photonic crystals.

We have tested the method for a 1D two-layer periodic medium with a one-layer defect and observed a close to exponential convergence of computations of the defect frequencies with respect to the numbers N_1 and N_2 of bands retained in the expansion for the associated eigenvalue equation and for an auxiliary nonhomogeneous linear equation for the perturbation of the Maxwellian operator, respectively, and to the partition number K for the discrete integration in k within each band. An evaluated (based on the exponential convergence) precision of $\sim 0.1\%$ is reached with $K=8$ and $N_1=10$ and $N_2=80$ or $N_1=20$ and $N_2=100$ for frequencies near the middle of the first or of the third gap, respectively (see Table I). The computations with such size arrays can be performed within a few minutes of the CPU time on a desktop computer. Comparing results of these computations of the defect frequencies in the first three gaps with the exact (up to $10^{-10}\%$) results of the propagation matrix (analytical) method [14], we find that an actual error is at most two times greater than an evaluated (based on the exponential hypothesis) error of $\sim 0.1\%$.

We apply the method to a 2D square lattice of square dielectric rods in a dielectric background with a one-rod replacement defect and, again, observe a close to exponential convergence of computations of the defect frequencies with respect to the partition number K and to the truncation numbers N_1 and N_2. Computing defect frequencies in the first gap with controlled evaluated precision of $\sim 1\%$ at increasing values of the defect-medium dielectric contrast, we observe four branches of defect modes of various symmetries rising at the top of the gap and (eventually) vanishing at its bottom. An evaluated (based on the exponential convergence) precision of $\sim 1\%$ for frequencies near the middle of a gap is reached with $K=6$ and $N_1=5$ and $N_2=10$ for the first (doublet) branch, $N_1=10$ and $N_2=30$ for the second (singlet) branch, and $N_1=30$ and $N_2=60$ for the third (quasidoublet) branch (see Table I and Fig. 2). Such computations take from ~ 0.3 min (for the first branch) to ~ 1 min (for the second branch) to ~ 10 min (for the third branch) of real time on four processors of a parallel computer SGI Origin2000.

The data concerning the configuration of the primitive cell of the periodic medium and of the defect enter these resolvent method computations in the form of the unperturbed frequency spectrum and the matrix of perturbation of the Maxwellian operator with respect to the basis of Bloch eigenfunctions. These data are obtained based on the preliminary solution of the spectral problem for the periodic medium. Using the basis of analytically known eigenfunctions of an auxiliary periodic operator for the case of relatively small spacing between the rods of the 2D lattice (as described in Sec. A 3), the subsystem of Bloch eigenfunctions (and of the corresponding eigenvalues) of a size sufficient for obtaining the above results for the defect states can be computed with the precision of $\sim 1\%$ within a few minutes of the CPU time on an advanced desktop computer. Subsequent computations (as described in Sec. IV B 2) of the corresponding perturbation matrix for a symmetric defect take ~ 30 min of real time on eight processors of Origin2000.

In summary, the resolvent method developed and tested in this work allows high precision computations of the defect modes of H polarization in 2D photonic crystals within reasonable CPU time using widely available computer resources. This method can be extended to 3D photonic crystals.

ACKNOWLEDGMENTS

Effort of A. Figotin and V. Goren is sponsored by the Air Force Office of Scientific Research, Air Force Materials Command, USAF, under Grant No. F49620-99-1-0203.

APPENDIX

1. Compactness of *S* operator for the resolvent method

a. Schrödinger's spectral problem

Compactness of the corresponding S operator (see Sec. I),

$$\mathbf{S}(\lambda)=-(\mathcal{H}_0-\lambda\mathbf{I})^{-1}\mathcal{H}_1, \tag{A1}$$

where

$$\mathcal{H}_0 = -a\Delta + U_0(\vec{r}), \quad \mathcal{H}_1 = U_1(\vec{r}) \tag{A2}$$

($a>0$ is a constant) with localized (square-integrable) $U_1(\vec{r})$, can be shown based on the exponential decay in $|\vec{r}' - \vec{r}|$ (and square-integrability at $\vec{r}' = \vec{r}$) of the Green's function $G(\vec{r}', \vec{r})$ [the kernel of the integral representation of the resolvent $(\mathcal{H}_0 - \lambda \mathbf{I})^{-1}$]. Because of that [22],

$$\mathrm{Tr}(\mathbf{S}^\dagger \mathbf{S}) = \int d\vec{r}' \int d\vec{r} |G(\vec{r}', \vec{r})|^2 |U_1(\vec{r})|^2$$

$$< b \int d\vec{r} |U_1(\vec{r})|^2 < \infty, \tag{A3}$$

where $b>0$ is a constant [i.e., $\mathbf{S}$ is a Hilbert-Schmidt operator, see item (7) of list in Sec. A 2].

b. Maxwell's spectral problem

We restrict our analysis to H-field formulation of the spectral problem. (For E-field formulation, a Schrödinger's-like representation of the direct resolvent approach is possible, see Sec. I.) The unperturbed and the perturbed Maxwellian operators are

$$\mathbf{M}_0 = \vec{\nabla} \times \varepsilon_0^{-1}(\vec{r}) \vec{\nabla} \times \tag{A4}$$

and

$$\mathbf{M} = \vec{\nabla} \times \varepsilon^{-1}(\vec{r}) \vec{\nabla} \times, \tag{A5}$$

correspondingly, with a bounded positive function $\varepsilon_0(\vec{r})$ or $\varepsilon(\vec{r})$, and the perturbation operator is

$$\mathbf{M}_1 = \mathbf{M} - \mathbf{M}_0 = \vec{\nabla} \times \gamma(\vec{r}) \vec{\nabla} \times \tag{A6}$$

with a localized bounded function $\gamma(\vec{r}) = \varepsilon^{-1}(\vec{r}) - \varepsilon_0^{-1}(\vec{r})$.

We do the analysis in terms of a general 3D vector case but it also applies to 1D ($d=1$) or 2D ($d=2$) systems as in Secs. II A and II B where the spectral problem reduces to a scalar Maxwellian operator (see Sec. II C):

$$\mathbf{M} = -\nabla_{\mathbf{r}} \cdot \varepsilon^{-1}(\mathbf{r}) \nabla_{\mathbf{r}}, \tag{A7}$$

$$\mathbf{r} = x\mathbf{e}_x, \quad \nabla_{\mathbf{r}} = \mathbf{e}_x \partial_x \quad \text{for} \quad d=1, \tag{A8}$$

$$\mathbf{r} = x\mathbf{e}_x + y\mathbf{e}_y, \quad \nabla_{\mathbf{r}} = \mathbf{e}_x \partial_x + \mathbf{e}_y \partial_y \quad \text{for} \quad d=2. \tag{A9}$$

(i) Resolvent approach with the shift-inverse. When the resolvent method is applied to the spectral problem in terms of the shift inverse of the Maxwellian operator (see Sec. III A), the corresponding S operator can be expressed as follows [see Eq. (63)]:

$$\mathbf{S}(\mu) = (\mu + m_s)(\mathbf{M}_0 - \mu \mathbf{I})^{-1} (\mathbf{M}_0 + m_s \mathbf{I}) \mathbf{W}_1 \tag{A10}$$

(with μ in a gap of the spectrum of the unperturbed operator $\mathbf{M}_0$), where $m_s>0$ is a constant and [see Eqs. (67), (52), and (56)]

$$\mathbf{W}_1 = -(\mathbf{M} + m_s \mathbf{I})^{-1} \mathbf{M}_1 (\mathbf{M}_0 + m_s \mathbf{I})^{-1} \tag{A11}$$

is a perturbation of the shift inverse of the Maxwellian operator.

The operator $\mathbf{W}_1$ is a compact (moreover, Hilbert-Schmidt) operator [23,24,30]. It is sufficient to prove this for the case where the function

$$\tilde{\gamma}(\vec{r}) = \gamma(\vec{r}) \varepsilon_0(\vec{r}) \tag{A12}$$

is smooth. (Indeed [see [30] and items (4) and (5) of list in Sec. A 2 and Eqs. (A4)–(A6) of this paper], any function $\gamma(\vec{r})$ can by represented as a sum of a non-negative function and a nonpositive function, and any localized sign-definite function $\gamma(\vec{r})$ can be circumscribed by such localized function $\gamma_s(\vec{r})$ of the same sign that the corresponding function $\tilde{\gamma}_s(\vec{r})$ is smooth.) Then, we can extract a term with $\mathbf{M}_0$ from $\mathbf{M}_1$ [see Eqs. (A4), (A6), and (A12)],

$$\mathbf{M}_1 = \tilde{\gamma}(\vec{r}) \mathbf{M}_0 + (\vec{\nabla} \tilde{\gamma}(\vec{r})) \times \varepsilon_0^{-1}(\vec{r}) \vec{\nabla} \times, \tag{A13}$$

and obtain

$$\mathbf{W}_1 = -(\mathbf{M} + m_s \mathbf{I})^{-1} \tilde{\gamma}(\vec{r}) \mathbf{M}_0 (\mathbf{M}_0 + m_s \mathbf{I})^{-1}$$

$$-(\mathbf{M} + m_s \mathbf{I})^{-1} (\vec{\nabla} \tilde{\gamma}(\vec{r})) \times \varepsilon_0^{-1}(\vec{r}) \vec{\nabla} \times (\mathbf{M}_0 + m_s \mathbf{I})^{-1}. \tag{A14}$$

Both summands in $\mathbf{W}_1$ are Hilbert-Schmidt operators [30] because [see items (9) and (10) of list in Sec. A 2] each of them is a product of a Hilbert-Schmidt operator and a bounded operator. The Hilbert-Schmidt factors are of the form

$$\mathbf{C}_1 = -(\mathbf{M} + m_s \mathbf{I})^{-1} \varphi(\vec{r}) \tag{A15}$$

with a localized bounded function $\varphi(\vec{r}) = \tilde{\gamma}(\vec{r})$ in the first summand or $\varphi(\vec{r}) = (\vec{\nabla} \tilde{\gamma}(\vec{r})) \varepsilon_0^{-1/2}(\vec{r})$ in the second summand. Such an operator $\mathbf{C}_1$ is a Hilbert-Schmidt operator, similarly to S operator for Schrödinger's problem [see Eq. (A1) with (A2)]; this can be shown based on the exponential decay (and square integrability) of the Green's function for the resolvent $(\mathbf{M} - \lambda \mathbf{I})^{-1}$ (see [24,32] for 3D vector case, or [33] for 1D or 2D scalar case). The remaining factor in the first summand,

$$\mathbf{B}_1 = \mathbf{M}_0 (\mathbf{M}_0 + m_s \mathbf{I})^{-1} \tag{A16}$$

is obviously bounded because [see item (11) of list in Sec. A 2] the spectrum of $\mathbf{M}_0$ is non-negative. The remaining factor in the second summand

$$\mathbf{B}_2 = \varepsilon_0^{-1/2}(\vec{r}) \vec{\nabla} \times (\mathbf{M}_0 + m_s \mathbf{I})^{-1} \tag{A17}$$

is also bounded because [see items (11) and (12) of list in Sec. A 2], accounting $(\vec{\nabla} \times)^\dagger = \vec{\nabla} \times$,

$$\mathbf{B}_2^\dagger \mathbf{B}_2 = (\mathbf{M}_0 + m_s \mathbf{I})^{-1} \mathbf{M}_0 (\mathbf{M}_0 + m_s \mathbf{I})^{-1} = \mathbf{M}_0 (\mathbf{M}_0 + m_s \mathbf{I})^{-2} \tag{A18}$$

is obviously bounded for non-negative $\mathbf{M}_0$.

Finally, operator $\mathbf{S}$ is compact (moreover, Hilbert-Schmidt) operator [see items (10) and (11) of list in Sec. A 2] being a product of a bounded operator $(\mu+m_s)(\mathbf{M}_0+m_s\mathbf{I})(\mathbf{M}_0-\mu\mathbf{I})^{-1}$ and a Hilbert-Schmidt operator $\mathbf{W}_1$.

(ii) Direct resolvent approach. If one tries to apply the resolvent method directly to the Maxwellian operator, the corresponding S operator (see Sec. I) would be

$$\mathbf{S}(\lambda)=-(\mathbf{M}_0-\lambda\mathbf{I})^{-1}\mathbf{M}_1, \tag{A19}$$

which is not compact. To prove this, it is enough to consider the case of a smooth function $\tilde{\gamma}(\vec{r})$ (A12), where we can extract the term with $\mathbf{M}_0$ from $\mathbf{M}_1$ [see Eq. (A13)] and, representing $\mathbf{M}_0=(\mathbf{M}_0-\lambda\mathbf{I})+\lambda\mathbf{I}$, obtain

$$\mathbf{S}^{\dagger}(\lambda)=-\mathbf{M}_1(\mathbf{M}_0-\lambda\mathbf{I})^{-1}=-\tilde{\gamma}(\vec{r})\mathbf{I}-\lambda\tilde{\gamma}(\vec{r})(\mathbf{M}_0-\lambda\mathbf{I})^{-1}$$
$$-(\vec{\nabla}\tilde{\gamma}(\vec{r}))\times\varepsilon_0^{-1}(\vec{r})\vec{\nabla}\times(\mathbf{M}_0-\lambda\mathbf{I})^{-1}. \tag{A20}$$

The first summand in $\mathbf{S}^{\dagger}$ is an operator of multiplication by a function and is not compact because [see item (3) of list in Sec. A 2] it has continuous spectrum. Therefore, the operator $\mathbf{S}$ as a whole is not compact (as stated in [23,24]), because (see items 4 and 6 of list in Sec. A2) the remainder of the sum is a compact operator.

Indeed, the second summand in $\mathbf{S}^{\dagger}$,

$$\mathbf{C}_2=-\lambda\tilde{\gamma}(\vec{r})(\mathbf{M}_0-\lambda\mathbf{I})^{-1} \tag{A21}$$

with a localized bounded function $\tilde{\gamma}(\vec{r})$, is similar to the operator $\mathbf{C}_1$ (A15) (with an arbitrary λ in a gap of $\mathbf{M}_0$ instead of $\lambda=-m_s$) compactness of which is discussed in Sec. A1bi.

The third summand in $\mathbf{S}^{\dagger}$,

$$\mathbf{C}_3=-\varepsilon_0^{-1}(\vec{r})(\vec{\nabla}\tilde{\gamma}(\vec{r}))\times\vec{\nabla}\times(\mathbf{M}_0-\lambda\mathbf{I})^{-1}, \tag{A22}$$

is also compact (as stated in [23]). Indeed [see item (8) of list in Sec. A 2], accounting that $[(\vec{\nabla}\tilde{\gamma}(\vec{r}))\times\vec{\nabla}\times]^{\dagger}=-\vec{\nabla}\times(\vec{\nabla}\tilde{\gamma}(\vec{r}))\times$,

$$\mathbf{C}_3^{\dagger}\mathbf{C}_3=-(\mathbf{M}_0-\lambda\mathbf{I})^{-1}\vec{\nabla}\times(\vec{\nabla}\tilde{\gamma}(\vec{r}))\times\varepsilon_0^{-2}(\vec{r})(\vec{\nabla}\tilde{\gamma}(\vec{r}))\times\vec{\nabla}$$
$$\times(\mathbf{M}_0-\lambda\mathbf{I})^{-1} \tag{A23}$$

is a Hilbert-Schmidt operator as it is of the same type as the operator $\mathbf{W}_1$ [see Eq. (A11) with (A6)] of perturbation of the shift inverse of the Maxwellian operator [see Sec. A 1 b (i)], with a localized bounded tensor function $\varepsilon_0^{-2}(\vec{r})(\vec{\nabla}\tilde{\gamma}(\vec{r}))\times(\vec{\nabla}\tilde{\gamma}(\vec{r}))\times$ in place of the scalar function $\gamma(\vec{r})$ (and with an arbitrary λ in a gap of $\mathbf{M}_0$ instead of $\lambda=-m_s$).

2. Compact and bounded operators in Hilbert space

We list here some statements of the general theory of linear operators (see, e.g., [34,35]), to which we refer in our analysis of the resolvent method.

(1) Every compact operator is a normwise limit of a sequence of finite rank operators.

(2) For any compact operator $\mathbf{C}$ its reduction to an N-dimensional subspace $\mathcal{L}_N$ converges normwise to the operator itself as $N\to\infty$ and $\mathcal{L}_N$ becomes the entire space,

$$\mathbf{P}_N\mathbf{C}\mathbf{P}_N\to\mathbf{C} \quad \text{as} \quad \mathbf{P}_N\to\mathbf{I}, \tag{A24}$$

where $\mathbf{P}_N$ is the projector on $\mathcal{L}_N$. (This follows from item 1 above, accounting that the property (A24) holds for any finite rank operator in place of $\mathbf{C}$).

(3) Spectrum of any compact operator is discrete with finite multiplicity of each nonzero eigenvalue and with zero being the only possible limit point of the spectrum.

(4) Linear combination of two compact operators is a compact operator.

(5) An operator confined between zero and a compact operator is also compact.

(6) An operator adjoint to a compact operator is also compact.

(7) If $\mathrm{Tr}(\mathbf{C}^{\dagger}\mathbf{C})^p<\infty$ with $p\geqslant 1$, then the operator $\mathbf{C}$ is compact. In particular, if $p=2$ then such $\mathbf{C}$ is called a Hilbert-Schmidt operator.

(8) If the operator $\mathbf{C}^{\dagger}\mathbf{C}$ is a Hilbert-Schmidt operator, then the operator $\mathbf{C}$ is compact. (This follows from item 7 above with $p=4$).

(9) An operator $\mathbf{B}$ is bounded if $(\mathbf{B}\psi,\mathbf{B}\psi)<b(\psi,\psi)$ for all ψ with some constant $b>0$ independent of ψ.

(10) Product of a compact operator and a bounded operator is compact.

(11) A self-adjoint operator is bounded if its spectrum is bounded.

(12) If the operator $\mathbf{B}^{\dagger}\mathbf{B}$ is bounded, then the operator $\mathbf{B}$ is also bounded.

3. Solution of the spectral problem for the rectangular geometry 2D periodic medium

We solve the spectral problem (35) for a 2D periodic medium of the type (96), following the method developed in [28,29]. If the thickness L_2^{α} of each wall of the grid is much smaller then the corresponding dimension L_1^{α} of the rod,

$$\Lambda^{\alpha}=L_2^{\alpha}/L_1^{\alpha}\ll 1, \tag{A25}$$

then the Maxwellian operator $\mathbf{M}_0$ (32) with (96) is relatively close [in the functional sense (30)] to the following auxiliary operator $\tilde{\mathbf{M}}_0$:

$$\tilde{\mathbf{M}}_0=-\sum_{\alpha=x,y}\partial_{\alpha}\frac{1}{\varepsilon_0^{\alpha}(r_{\alpha})}\partial_{\alpha}, \tag{A26}$$

where

$$\varepsilon_0^{\alpha}(r_{\alpha})=\epsilon_1, \quad r_{\alpha}\in(0,L_1^{\alpha}),$$
$$\varepsilon_0^{\alpha}(r_{\alpha})=\epsilon_2, \quad r_{\alpha}\in(L_1^{\alpha},L_{\alpha}). \tag{A27}$$

Therefore, the system of eigenfunctions $\{\tilde{\psi}_0(x,y)\}$ of the operator $\tilde{\mathbf{M}}_0$,

$$\tilde{\mathbf{M}}_0\tilde{\psi}_0(x,y)=\tilde{m}_0\tilde{\psi}_0(x,y), \tag{A28}$$

can be taken as a basis for the representation of the spectral problem for $\mathbf{M}_0$ allowing an efficient iterative numerical solution.

Because the operator $\tilde{\mathbf{M}}_0$ is periodic in x and y (with the same periods L_x and L_y as the operator $\mathbf{M}_0$), all analysis of the Sec. II D concerning the structure of the spectral system applies to $\tilde{\mathbf{M}}_0$. The operator $\tilde{\mathbf{M}}_0$ is a direct sum of two one-dimensional operators $\mathbf{M}_0^\alpha$ ($\alpha=x,y$), each of the same form as the operator $\mathbf{M}_0$ for the 1D periodic medium studied in Sec. IV A 1 [compare Eq. (A26) with Eq. (A27) to Eq. (32) for $d=1$ with Eq. (80)]:

$$\tilde{\mathbf{M}}_0=\sum_{\alpha=x,y}\mathbf{M}_0^\alpha,\quad \mathbf{M}_0^\alpha=-\partial_\alpha\frac{1}{\varepsilon_0^\alpha(r_\alpha)}\partial_\alpha. \tag{A29}$$

Due to this, the system of Bloch eigenfunctions of the operator $\tilde{\mathbf{M}}_0$ can be found as direct product of the systems of Bloch eigenfunctions of the two operator summands [see Eqs. (36) and (37)]:

$$\tilde{\psi}_{0\mathbf{n},\mathbf{k}}(x,y)=\prod_{\alpha=x,y}\psi^\alpha_{0n_\alpha,k_\alpha}(r_\alpha), \tag{A30}$$

$$\mathbf{n}=(n_x,n_y),\quad n_\alpha=1,2,\ldots,\infty,\quad k_\alpha\in[-\pi,\pi], \tag{A31}$$

where the function $\psi^\alpha_{0n,k}(r_\alpha)$ is given by the formulas (86)–(89) with $L^\alpha_{1,2}$ in place of $L_{1,2}$ (and r_α in place of x). Each corresponding eigenvalue is a sum of the eigenvalues associated with the factors $\psi^\alpha_{0n_\alpha,k_\alpha}(r_\alpha)$ [see Eq. (82)]:

$$\tilde{m}_0(\mathbf{n},\mathbf{k})=\sum_{\alpha=x,y}(\nu^\alpha_{0n_\alpha}(k_\alpha)/n_1L_1^\alpha)^2, \tag{A32}$$

where the function $\nu^\alpha_{0n}(k)$ is determined by the equation (84) with $L^\alpha_{1,2}$ in place of $L_{1,2}$ in Eq. (85). Orthonormality of the basis system $\{\psi_{0n,k}(x)\}$ in $L^2(\mathrm{R})$ for $d=1$ yields orthonormality of the basis system $\{\tilde{\psi}_{0\mathbf{n},\mathbf{k}}(x,y)\}$ in $L^2(\mathrm{R}^2)$ for $d=2$ [see (50)]:

$$(\tilde{\psi}_{0\mathbf{n},\mathbf{k}},\tilde{\psi}_{0\mathbf{n}',\mathbf{k}'})=\delta_{\mathbf{n},\mathbf{n}'}\delta(\mathbf{k}-\mathbf{k}'). \tag{A33}$$

We can reenumerate the subsystem (A30) of Bloch eigenfunctions of the operator $\tilde{\mathbf{M}}_0$ for each fixed $\mathbf{k}$ to have the corresponding eigenvalues (A32) in ascending order:

$$\{\tilde{\psi}_{0\mathbf{n},\mathbf{k}},\tilde{m}_0(\mathbf{n},\mathbf{k})\mid n_{x,y}=1,2,\ldots,\infty\}\equiv\{\tilde{\psi}_{0n,\mathbf{k}},\tilde{m}_0(n,\mathbf{k})\mid n=1,2,\ldots,\infty\} \tag{A34}$$

$$\tilde{m}_0(n+1,\mathbf{k})\geqslant\tilde{m}_0(n,\mathbf{k}), \tag{A35}$$

where n enumerates all different pairs (n_x,n_y) in the order of ascend of the eigenvalues $\tilde{m}_0(n_x,n_y;\mathbf{k})$, counting each multiple eigenvalue (if any) the number of times (in a row) equal to its multiplicity [compare this to the general structure (46) with (47)]. There may be some multiple eigenvalues due to some extra symmetry. For example, if $L^x_{1,2}=L^y_{1,2}$ then $\tilde{m}_0(n,n';k,k)=\tilde{m}_0(n',n;k,k)$ [see Eq. (A32)].

Because the operators $\mathbf{M}_0$ and $\tilde{\mathbf{M}}_0$ are periodic in x and y with the same periods L_x and L_y, respectively, the subsystem (A34) of Bloch eigenfunctions of the operator $\tilde{\mathbf{M}}_0$ for each fixed $\mathbf{k}$ can be used as such orthogonal basis [see Eq. (48)] for the representation of the eigenvalue equation (40) with (41) for the operator $\mathbf{M}_0$ in $L^2(Q)$ that the Bloch boundary conditions (42) will be automatically satisfied for that $\mathbf{k}$. Then, each eigenfunction $\psi_{0\mathbf{k}}(x,y)$ of $\mathbf{M}_0$ represents with its Fourier coefficients $\{b_\mathbf{k}(n)\}_n$,

$$\psi_{0\mathbf{k}}(x,y)=\sum_{n=1}^{\infty}b_\mathbf{k}(n)\tilde{\psi}_{0n,\mathbf{k}}(x,y), \tag{A36}$$

where [see Eq. (48)]

$$b_\mathbf{k}(n)=C_2^{-1}(\tilde{\psi}_{0n,\mathbf{k}}|\psi_{0\mathbf{k}})_Q, \tag{A37}$$

and the equation (40) represents with the following system of algebraic equations for the coefficients $\{b_\mathbf{k}(n)\}_n$:

$$\sum_{n'=1}^{\infty}M_{0\mathbf{k}}(n,n')b_\mathbf{k}(n')=m_0(\mathbf{k})b_\mathbf{k}(n),\quad n=1,2,\ldots,\infty, \tag{A38}$$

where the matrix,

$$M_{0\mathbf{k}}(n,n')=C_2^{-1}(\tilde{\psi}_{0n,\mathbf{k}},\mathbf{M}_0\tilde{\psi}_{0n',\mathbf{k}})_Q \tag{A39}$$

$$=4\pi^2\int_0^{L_x}dx\int_0^{L_y}dy\,\frac{1}{\varepsilon_o(x,y)}\times\sum_{\alpha=x,y}(\partial_\alpha\tilde{\psi}^*_{0n,\mathbf{k}}(x,y))\times(\partial_\alpha\tilde{\psi}_{0n',\mathbf{k}}(x,y)) \tag{A40}$$

[see Eqs. (48), (32), (45), (36), and (13)], can be computed analytically [see Eqs. (A30) and (96)].

The system (A38) represents the eigenvalue problem for the matrix $M_{0\mathbf{k}}(n,n')$ $(n,n'=1,2,\ldots,\infty)$ with an infinite discrete system of eigenvectors $\{b_\mathbf{k}(n')\}_{n'}$ and corresponding eigenvalues $m_0(\mathbf{k})$:

$$\{\{b_{n,\mathbf{k}}(n')\}_{n'=1}^{\infty},m_0(n,\mathbf{k})\}\quad(n=1,2,\ldots,\infty). \tag{A41}$$

Because each of the two systems of eigenfunctions, $\{\psi_{0n,\mathbf{k}}\}_n$ and $\{\tilde{\psi}_{0n,\mathbf{k}}\}_n$, is orthogonal and both have the same fixed norm [see Eq. (48)], the relation (A36) implies that the system (A41) of eigenvectors $\{b_\mathbf{k}(n)\}_n$ is orthonormal:

$$\sum_{n=1}^{\infty} b_{n',\mathbf{k}}(n) b_{n'',\mathbf{k}}(n) = \delta_{n',n''}. \tag{A42}$$

The infinite system of homogeneous equations (A38) is solved iteratively. Truncating the summation in n with a number N_3, we obtain the eigenvalue problem for the finite matrix $\{M_{0\mathbf{k}}(n,n')\}$ $(n,n'=1,2,\ldots,N_3)$ and solve it using a specialized standard library routine, obtaining the system of N_3 eigenvectors with corresponding eigenvalues. We increase N_3 (starting with $N_3=N_2$) until reaching necessary precision for the system of the first N_2 eigenvalues and corresponding eigenvectors, which is needed for the application of the resolvent method (see Sec. III C); the precision for a vector $\{b_{n,\mathbf{k}}(n')\}_{n'}$ can be evaluated based on the norm of the difference between iteration results (completed with zero components for smaller N_3). Due to closeness [in the functional sense (30)] of the operators $\mathbf{M}_0$ and $\tilde{\mathbf{M}}_0$ [under the condition (A25)], we can expect that reasonable precision for the eigenvalues and eigenvectors can be reached with a moderate truncation number N_3 (for example, $N_3 \sim 10N_2$). Then, the corresponding approximation for each eigenfunction of the operator $\mathbf{M}_0$ represented with an eigenvector $\{b_{n,\mathbf{k}}(n')\}_{n'}$ can be obtained by summation (A36) truncated with the same number N_3:

$$\psi_{0n,\mathbf{k}}(x,y) \approx \sum_{n'=1}^{N_3} b_{n,\mathbf{k}}(n') \tilde{\psi}_{0n',\mathbf{k}}(x,y), \quad n=1,2,\ldots,N_2. \tag{A43}$$

[1] *Photonic Band Gaps and Localization*, edited by C. M. Soukoulis (Plenum, New York, 1993).

[2] J. Opt. Soc. Am. B **10** (1993), special issue on development and application of materials exhibiting photonic band gaps, edited by C.M. Bowden, J.P. Dowling, and H.O. Everitt.

[3] J. Mod. Opt. **41** (1994), special issue on photonic band structures, edited by G. Kurizki and J.W. Haus.

[4] *Photonic Band Gap Materials*, edited by C. M. Soukoulis (Kluwer Academic, Dordrecht, 1996).

[5] *Microcavities and Photonic Bandgaps*, edited by J. Rarity and C. Weisbuch (Kluwer Academic, Dordrecht, 1996).

[6] E. Yablonovitch, in *Photonic Band Structures* (Ref. [3]), pp. 173–194.

[7] J.W. Haus, in *Photonic Band Structures* (Ref. [3]), pp. 195–207.

[8] E. Yablonovitch, T.J. Gmitter, R.D. Meade, A.M. Rappe, K.D. Brommer, and J.D. Joannopoulos, Phys. Rev. Lett. **67**, 3380 (1991).

[9] D.R. Smith, R. Dalichaouch, N. Kroll, S. Schultz, S.L. McCall, and P.M. Platzman, in *Development and Application of Materials Exhibiting Photonic Band Gaps* (Ref. [2]), pp. 314–322.

[10] S. Schultz and D.R. Smith, in *Photonic Band Gaps and Localization* (Ref. [1]), pp. 305–316.

[11] D.R. Smith, S. Schultz, S.L. McCall, and P.M. Platzman, in *Photonic Band Structures* (Ref. [3]), pp. 395–404.

[12] J.D. Jackson, *Classical Electrodinamics* (John Wiley, New York, 1975).

[13] K. Busch, C.T. Chan, and C.M. Soukoulis, in *Photonic Band Gap Materials* (Ref. [4]), pp. 465–485.

[14] A. Figotin and V. Gorentsveig, Phys. Rev. B **58**, 180 (1998).

[15] R.D. Meade, K.D. Brommer, A.M. Rappe, and J.D. Joannopoulos, Phys. Rev. B **44**, 13 772 (1991).

[16] R.D. Meade, A.M. Rappe, K.D. Brommer, J.D. Joannopoulos, and O.L. Alerhand, Phys. Rev. B **48**, 8434 (1993).

[17] K. Sakoda and H. Shiroma, Phys. Rev. B **56**, 4830 (1997).

[18] K. Sakoda, J. Appl. Phys. **84**, 1210 (1998).

[19] V. Kuzmiak and A.A. Maradudin, Phys. Rev. B **57**, 15 242 (1998).

[20] M. Qiu and S. He, Phys. Rev. B **61**, 12 871 (2000).

[21] A.M. Zheltikov, S.A. Magnitskii, and A.V. Tarasishin, J. Exp. Theor. Phys. **90**, 600 (2000).

[22] M. Reed and B. Simon, *Methods of Modern Mathematical Physics* (Academic Press, New York, 1978), Vol. IV.

[23] A. Figotin and A. Klein, SIAM (Soc. Ind. Appl. Math.) J. Appl. Math. **58**, 1748 (1998).

[24] A. Figotin and A. Klein, J. Opt. Soc. Am. **15**, 1423 (1998).

[25] A.A. Maradudin and A.R. McGurn, in *Photonic Band Gaps and Localization* (Ref. [1]), pp. 247–268.

[26] M.G. Khazhinsky and A.R. McGurn, Phys. Lett. A **237**, 175 (1998).

[27] K.M. Leung, in *Development and Application of Materials Exhibiting Photonic Band Gaps* (Ref. [2]), pp. 303–306.

[28] A. Figotin and P. Kuchment, SIAM (Soc. Ind. Appl. Math.) J. Appl. Math. **56**, 1561 (1996).

[29] A. Figotin and Yu. Godin, J. Comput. Phys. **136**, 585 (1997).

[30] A. Figotin and A. Klein, J. Stat. Phys. **86**, 165 (1997).

[31] A. Abragam and B. Bleney, *Electron Paramagnetic Resonance of Transition Ions* (Clarendon, Oxford, 1970).

[32] A. Figotin and A. Klein, Commun. Math. Phys. **184**, 411 (1997).

[33] A. Figotin and A. Klein, Commun. Math. Phys. **180**, 439 (1996).

[34] M. Reed and B. Simon, *Methods of Modern Mathematical Physics* (Academic Press, New York, 1972), Vol. I.

[35] N.I. Akhiezer and I.M. Glazman, *Theory of Linear Operators in Hilbert Space* (Dover, New York, 1993).

[36] Opt. Express **8** (2001), focus issue on photonic bandgap calculations, edited by M. de Sterke and K. Busch.